PERGAMON

International Journal of Solids and Structures 38 (2001) 6665–6697

INTERNATIONAL JOURNAL OF SOLIDS and STRUCTURES

www.elsevier.com/locate/ijsolstr

Mathematical model of delamination cracks on imperfect interfaces

Y.A. Antipov [a], O. Avila-Pozos [a], S.T. Kolaczkowski [b], A.B. Movchan [c,*]

[a] *Department of Mathematical Sciences, University of Bath Claverton Down, Bath BA2 7AY, UK*
[b] *Department of Chemical Engineering, University of Bath Claverton Down, Bath BA2 7AY, UK*
[c] *Department of Mathematical Sciences, University of Liverpool, Liverpool L69 3BX, UK*

Received 12 April 1999

Abstract

A mathematical model of a crack along a thin and soft interface layer is studied in this paper. This type of interface could arise in a ceramic support that has been coated with a layer of high surface area material which contains the dispersed catalyst. Asymptotic analysis is applied to replace the interface layer with a set of effective contact conditions. We use the words "imperfect interface" to emphasise that the solution (the temperature or displacement field) is allowed to have a non-zero jump across the interface. Compared to classical formulations for cracks in dissimilar media (where ideal contact conditions are specified outside the crack), in our case the gradient field for the temperature (or displacement) is characterised by a weak logarithmic singularity. The scalar case for the Laplacian operator as well as the vector elasticity problem are considered. Numerical results are presented for a two-phase elastic strip containing a finite crack on an imperfect interface.

Keywords: Imperfect interfaces; Delamination cracks; Mathematical model

1. Introduction

Motivation for this work arises from the study of the fracture of ceramic catalytic monolith combustors that are being incorporated into new prototype designs of gas turbines. The possibility of crack propagation in the ceramic support and methods of calculations have already been described in Antipov et al. (1999). The ceramic monolith consists of an extruded structure that contains a large number of parallel channels, e.g. consisting of: 62 cells/cm^2; each cell 1.1×1.1 mm^2 square; with an open frontal area of 66%. The ceramic surface is coated with a high surface area material (e.g. γ-Al_2O_3) which contains the dispersed catalyst. It is in the catalytic layer (also known as the washcoat), where the combustion reactions take place (e.g. $CH_4 + 2O_2 \rightarrow CO_2 + 2H_2O$), and the energy associated with this highly exothermic reaction is released. In the application in a gas turbine combustor, temperatures of the catalyst layer could vary from ambient conditions (when the turbine is not working) up to 1100°C. It is important that the catalyst layer

* Corresponding author. Tel.: +44-151-794-4740; fax: +44-151-794-4061.
E-mail addresses: masya@maths.bath.ac.uk (Y.A. Antipov), abm@liv.ac.uk (A.B. Movchan).

0020-7683/01/$ - see front matter
PII: S0020-7683(01)00027-0

remains firmly bound to the ceramic support structure during this process. If it cracks and shears, then catalyst will be lost from the monolith which would (a) result in a lost in performance of the combustor, and (b) lead to possible damage of components downstream of the combustor. Further information on catalytic combustion and the use of ceramic monolith supports is available in Hayes and Kolaczkowski (1997). Asymptotic study of cracks in a cellular structure of a catalytic monolith combustor is included in Antipov et al. (2000).

As the surface of the monolith is covered by a layer of catalyst, this gives a two-phase structure. A scanning electron micrograph (SEM) of the face of a catalyst coated channel is illustrated in Fig. 1, taken at a tilt angle of 15° to view the surface of the catalyst layer. In examining the surface, cracks are clearly visible in the layer. The cracks would have occurred as a result of (a) shrinkage of the coated layer (after drying and calcining), and (b) differences in coefficients of thermal expansion as the material was exposed to a wide range of temperatures. The presence of a crack on the surface is not considered necessarily to be a problem, however, if the crack propagates and the interface is sheared then this will lead to catalyst loss.

It is documented in engineering literature that the damage of ceramic structures is accompanied by "crack bridging". In the model presented here we assume that the bridging effect exists along the whole interface surface between the substrate and the layer of catalyst (often, we shall also use the words "imperfect interface" or "soft adhesive"), and, in addition, a crack with zero tractions on its faces is introduced along the interface contour. We study the problems of heat transfer (or anti-plane shear) and elasticity problems for this two-phase structure.

Mathematical models of interfacial cracks are well developed in the literature for the cases when ideal contact conditions prevail on an interface surface outside a crack. Plane problems for cracks in dissimilar media were studied by Rice and Sih (1965) and by England (1965). The work of Willis (1971) introduces the integral equation approach for analysis of interfacial cracks including the cases of three-dimensions and dynamic cracks. Asymptotic models of elastic adhesive joints were introduced by Klarbring (1991), Klarbring and Movchan (1995, 1998) and Avila-Pozos et al. (1999). The adhesive was modelled as a thin and soft layer where effective contact conditions involve continuity of tractions and a linear relation between the traction components and the displacement jump across the adhesive. Laminated structures with linear interfaces were also studied by Bigoni et al. (1997).

In the present work we analyse mathematical models of cracks along imperfect interface boundaries and make an emphasis on the asymptotic behaviour of the solution and its derivatives near the crack ends and at infinity. In contrast to the results already published in the literature, on the interface boundary (outside the crack) we allow for a non-zero displacement jump specified as a function of traction components. The presence of this condition affects the asymptotics of the displacement and stress components in the vicinity of the crack ends.

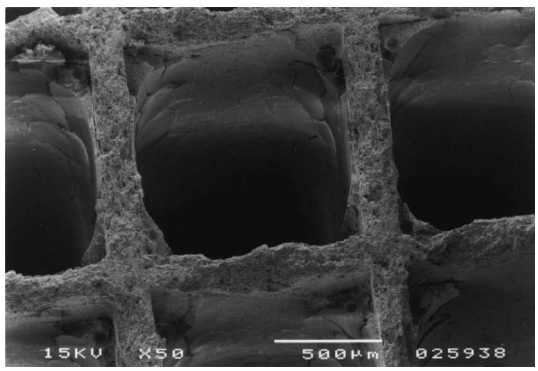

Fig. 1. SEM of a face of a catalyst coated monolith (photograph supplied courtesy of University of Bath, UK).

The structure of the paper can be described as follows:

In Section 2 we discuss the asymptotic model of a thin and soft layer (adhesive) and derive effective interface conditions.

Section 3 presents an exact solution of the Dirichlet problem for the Laplacian for a strip containing a semi-infinite crack along the imperfect interface. In terms of physical applications, this model corresponds to the heat transfer problem for a strip with temperature prescribed on the upper and lower parts of the surface, zero flux at the crack boundary, and a flux proportional to the temperature difference ahead of the crack. Alternatively, this model can be interpreted as the anti-plane shear problem of elasticity with a thin and soft layer of adhesive placed ahead of the interfacial crack. The problem is reduced to a scalar Wiener–Hopf functional equation that is solved exactly. The behaviour of the solution at the end of the crack is found by the same technique that was used by Antipov (1993). The method is based on the asymptotic expansion of the integral representation of the solution and on Abelian type theorems. Analysis shows that the temperature gradient (or shear stress for the elasticity model) has a logarithmic singularity at the crack tip. At the same time, the normal derivative of the temperature is bounded and discontinuous at the crack tip along the interface and the tangential derivative tends to infinity as a logarithmic function. It is known that for the case of ideal contact ahead of the crack, the singularity is much stronger: the temperature gradient components have the order $O(r^{-1/2})$, as the distance r to the crack tip tends to zero. At infinity, the solution decays exponentially.

In Section 4 we study the Neumann boundary value problem for the domain of the same configuration as above. The qualitative structure of the asymptotics in the vicinity of the crack tip does not change. However, the behaviour of the solution at infinity is different from the case when the temperature values are specified on the upper and lower parts of the boundary of the strip. The exact solution is found by the factorisation method. Explicit asymptotic formulae for the temperature jump are obtained when $x \to \pm\infty$. It is shown that the temperature jump decays exponentially at infinity along the interface outside the crack and is bounded at infinity along the crack.

In Section 5 we analyse a solution of the model problem in a semi-infinite crack in a two-phase plane with the phases being separated by a line of imperfect interface. In contrast with previous sections, it is shown that the solution is characterised by algebraic asymptotics at infinity.

After the analysis of exact solutions obtained for the case of boundary value problems formulated for the Laplace operator, we turn to a plane strain problem for a two-phase elastic strip with a finite crack along an imperfect interface in Section 6. The problem is formulated in terms of a system of singular integral equations. An accurate numerical algorithm is proposed and implemented to obtain the values of the displacement components and stress in a neighbourhood of the crack. The stress components are shown to be bounded in the vicinity of the crack ends.

Numerical results are discussed in Section 7.

2. Asymptotic model of adhesive joints

Consider two bodies Ω_+ and Ω_- connected through a thin interface layer Ω_0 of thickness ϵ (see Fig. 2). Assume that the material occupying Ω_+, Ω_- and Ω_0 is characterised by the shear moduli μ_+, μ_- and $\mu_0 = \epsilon\mu$ respectively, where μ is of the same order as μ_+ and μ_-.

2.1. Anti-plane shear

For the case of anti-plane shear, we consider the displacement field $(0, 0, u(x, y))$ with the only non-zero component being the z-component, which depends on x and y only. The displacements u^+, u^- and $u^{(0)}$ in Ω_+, Ω_- and Ω_0 satisfy the following equations

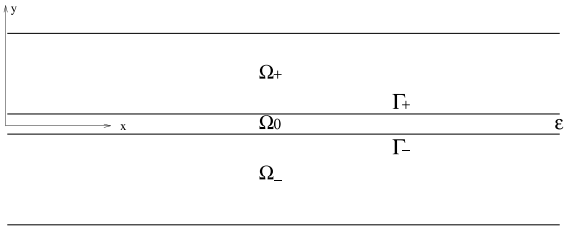

Fig. 2. The adhesive joint.

$$\nabla^2 u^{\pm} = 0 \quad \text{in } \Omega_{\pm}, \tag{2.1}$$

$$\nabla^2 u^{(0)} = 0 \quad \text{in } \Omega_0 \tag{2.2}$$

and

$$u^{+} = u^{(0)}, \quad \mu_{+}\frac{\partial u^{+}}{\partial y} = \mu_0 \frac{\partial u^{(0)}}{\partial y} \quad \text{on } \Gamma_{+}, \tag{2.3}$$

$$u^{-} = u^{(0)}, \quad \mu_{-}\frac{\partial u^{-}}{\partial y} = \mu_0 \frac{\partial u^{(0)}}{\partial y} \quad \text{on } \Gamma_{-}, \tag{2.4}$$

where

$$\Gamma_{+} = \{(x,y):\ y = \epsilon/2\},$$

$$\Gamma_{-} = \{(x,y):\ y = -\epsilon/2\}.$$

Let $t = \epsilon^{-1}y$, so that within Ω_0, $|y| < \epsilon/2$ and hence $|t| < 1/2$. In terms of x and t

$$\nabla^2 u^{(0)} = \epsilon^{-2}\frac{\partial^2 u^{(0)}}{\partial t^2} + \frac{\partial^2 u^{(0)}}{\partial x^2} = 0.$$

Let $u_0^{(0)}$ denote the leading term of $u^{(0)}$. Then

$$\frac{\partial^2 u_0^{(0)}}{\partial t^2} = 0 \quad \text{in } \Omega_0$$

and therefore

$$u_0^{(0)} = C_1^{(0)}(x) + tC_2^{(0)}(x),$$

with C_1, C_2 being functions of x only. Using the displacement contact conditions in Eqs. (2.3) and (2.4) we deduce

$$C_1^{(0)} = \tfrac{1}{2}(u^{+}(x_1,0) + u^{-}(x_1,0)),$$
$$C_2^{(0)} = u^{+}(x_1,0) - u^{-}(x_1,0)$$

and the traction contact conditions in Eqs. (2.3) and (2.4) yield

$$\mu_{\pm}\frac{\partial u^{\pm}}{\partial y}(x_1,0) = \mu\frac{\partial u_0^{(0)}}{\partial t} = \mu(u^{+}(x_1,0) - u^{-}(x_1,0))$$

to leading order. It is shown that the leading order term of tractions is continuous across the interface layer

$$T(x_1) := \mu_+ \frac{\partial u^+}{\partial y}(x_1, 0) = \mu_- \frac{\partial u^-}{\partial y}(x_1, 0) \tag{2.5}$$

and it is proportional to the displacement jump across the interface

$$T(x_1) = \mu(u^+(x_1, 0) - u^-(x_1, 0)). \tag{2.6}$$

In the text below, the quantity μ will be called the stiffness coefficient of the interface layer Ω_0.

2.2. Plane strain with isotropic interface layer

For the case of plane strain the materials occupying Ω_0 and $\Omega_\pm$ are characterised by the Lamé elastic moduli $\lambda_0 = \epsilon\lambda$, $\mu_0 = \epsilon\mu$ and $\lambda_\pm$, $\mu_\pm$, where λ, μ have the same order of magnitude as $\lambda_\pm$, $\mu_\pm$.

The displacements vectors $\boldsymbol{u}^\pm$ and $\boldsymbol{u}^{(0)}$ satisfy the Lamé equations of equilibrium

$$L_\pm(\boldsymbol{u}^\pm) = 0 \quad \text{in } \Omega_\pm, \tag{2.7}$$

$$L_0(\boldsymbol{u}^{(0)}) = 0 \quad \text{in } \Omega_0, \tag{2.8}$$

where

$$L_\pm(\boldsymbol{u}) = \mu_\pm \nabla^2 \boldsymbol{u} + (\lambda_\pm + \mu_\pm)\nabla\nabla \cdot \boldsymbol{u}$$

and

$$L_0(\boldsymbol{u}^{(0)}) = \epsilon^{-2}\begin{pmatrix} \mu_0 & 0 \\ 0 & \lambda_0 + 2\mu_0 \end{pmatrix} \frac{\partial^2 \boldsymbol{u}^{(0)}}{\partial t^2} + \epsilon^{-1}\begin{pmatrix} 0 & \lambda_0 + \mu_0 \\ \lambda_0 + \mu_0 & 0 \end{pmatrix} \frac{\partial^2 \boldsymbol{u}^{(0)}}{\partial x\, \partial t} + \begin{pmatrix} \lambda_0 + 2\mu_0 & 0 \\ 0 & \mu_0 \end{pmatrix} \frac{\partial^2 \boldsymbol{u}^{(0)}}{\partial x^2}.$$

The interface contact conditions on $\Gamma_\pm$ have the form

$$\boldsymbol{u}^+ = \boldsymbol{u}^{(0)}, \quad \boldsymbol{\sigma}_+^{(2)}(\boldsymbol{u}^+) = \boldsymbol{\sigma}^{(2)}\big(\boldsymbol{u}^{(0)}\big) \quad \text{on } \Gamma_+, \tag{2.9}$$

$$\boldsymbol{u}^- = \boldsymbol{u}^{(0)}, \quad \boldsymbol{\sigma}_-^{(2)}(\boldsymbol{u}^-) = \boldsymbol{\sigma}^{(2)}\big(\boldsymbol{u}^{(0)}\big) \quad \text{on } \Gamma_- \tag{2.10}$$

where $\boldsymbol{\sigma}^{(2)} = (\sigma_{12}, \sigma_{22})^{\mathrm{T}}$. It follows from Eq. (2.8) that the leading term $\boldsymbol{u}_0^{(0)}$ of $\boldsymbol{u}^{(0)}$ is linear with respect to t

$$\boldsymbol{u}_0^{(0)} = \boldsymbol{C}_1^{(0)}(x) + t\boldsymbol{C}_2^{(0)}(x),$$

where the vector functions $\boldsymbol{C}_1^{(0)}$, $\boldsymbol{C}_2^{(0)}$ are defined from the displacement contact conditions in Eqs. (2.9) and (2.10)

$$\boldsymbol{C}_1^{(0)} = \tfrac{1}{2}(\boldsymbol{u}^+(x, 0) + \boldsymbol{u}^-(x, 0)), \quad \boldsymbol{C}_2^{(0)} = \boldsymbol{u}^+(x, 0) - \boldsymbol{u}^-(x, 0).$$

It follows from the traction conditions in Eqs. (2.9) and (2.10) that

$$\boldsymbol{\sigma}_+^{(2)}(\boldsymbol{u}^+)|_{(x,0)} = \boldsymbol{\sigma}_-^{(2)}(\boldsymbol{u}^-)|_{(x,0)} = \frac{1}{\epsilon}\begin{pmatrix} \mu_0 & 0 \\ 0 & \lambda_0 + 2\mu_0 \end{pmatrix} \frac{\partial \boldsymbol{u}_0^{(0)}}{\partial t} = \begin{pmatrix} \mu & 0 \\ 0 & \lambda + 2\mu \end{pmatrix}(\boldsymbol{u}^+(x, 0) - \boldsymbol{u}^-(x, 0)) \tag{2.11}$$

to leading order.

2.3. Plane strain with anisotropic interface layer

Here, we assume that the material in Ω_0 is anisotropic characterised by the constitutive relation

$$\begin{pmatrix} \sigma_{11}^0 \\ \sigma_{22}^0 \\ \sqrt{2}\sigma_{12}^0 \end{pmatrix} = \epsilon \begin{pmatrix} c_{11} & c_{12} & c_{13} \\ c_{12} & c_{22} & c_{23} \\ c_{13} & c_{23} & c_{33} \end{pmatrix} \begin{pmatrix} \epsilon_{11}^0 \\ \epsilon_{22}^0 \\ \sqrt{2}\epsilon_{12}^0 \end{pmatrix},$$

where $C \equiv (c_{ij})$ is the Hooke's matrix. The equations of equilibrium in Ω_0 have the form

$$D^{\mathrm{T}}\left(\frac{\partial}{\partial x}, \frac{\partial}{\partial y}\right) CD\left(\frac{\partial}{\partial x}, \frac{\partial}{\partial y}\right) \boldsymbol{u}^{(0)} = 0 \quad \text{in } \Omega_0,$$

where D is the matrix differential operator specified by

$$D\left(\frac{\partial}{\partial x}, \frac{\partial}{\partial y}\right) = \begin{pmatrix} \frac{\partial}{\partial x} & 0 \\ 0 & \frac{\partial}{\partial y} \\ \frac{1}{\sqrt{2}}\frac{\partial}{\partial y} & \frac{1}{\sqrt{2}}\frac{\partial}{\partial x} \end{pmatrix}.$$

Then the vector of tractions $\boldsymbol{\sigma}_0^{(2)}$ is

$$\boldsymbol{\sigma}_0^{(2)}(\boldsymbol{u}^{(0)}) = D^{\mathrm{T}}(0,1)CD\left(\frac{\partial}{\partial x}, \frac{\partial}{\partial y}\right)\boldsymbol{u}^{(0)} \sim \begin{pmatrix} \frac{1}{2}c_{33} & \frac{1}{\sqrt{2}}c_{23} \\ \frac{1}{\sqrt{2}}c_{23} & c_{22} \end{pmatrix} \frac{\partial \boldsymbol{u}^{(0)}}{\partial t}.$$

Similar to the previous (isotropic) case, we show that the leading term of $\boldsymbol{u}^{(0)}$ is linear in t, the tractions $\boldsymbol{\sigma}^{(2)}$ are continuous across the interface and depend linearly on the displacement jump, i.e.

$$\boldsymbol{\sigma}_+^{(2)}(\boldsymbol{u}^+)|_{(x,0)} = \boldsymbol{\sigma}_-^{(2)}(\boldsymbol{u}^-)|_{(x,0)} = \begin{pmatrix} \frac{1}{2}c_{33} & \frac{1}{\sqrt{2}}c_{23} \\ \frac{1}{\sqrt{2}}c_{23} & c_{22} \end{pmatrix} (\boldsymbol{u}^+(x,0) - \boldsymbol{u}^-(x,0)). \tag{2.12}$$

The relations (2.5), (2.6), (2.11) and (2.12) give the limit boundary conditions on the interface.

3. The Dirichlet problem for a strip with a semi-infinite crack along the imperfect interface

Here, we consider the problem of anti-plane shear for the case when the upper and lower sides of the strip are fixed and the crack surface is subject to given tractions. The alternative physical interpretation is related to distribution of temperature in the strip whose exterior surface is kept at a constant temperature, and the heat flux is specified on the crack faces.

3.1. Mathematical formulation

Let a three-phase strip contain a semi-infinite delamination crack. Ahead of the crack a thin layer of soft adhesive exists, and following the analysis of Section 2, it will be replaced by the discontinuity line where the jump in displacement is proportional to tractions (see Fig. 3). Formally, the problem is set as follows

$$\nabla^2 u(x,y) = 0, \quad |x| < \infty, \quad -b < y < 0, \quad 0 < y < a, \tag{3.1}$$

$$u(x,a) = u(x,-b) = 0, \quad |x| < \infty, \tag{3.2}$$

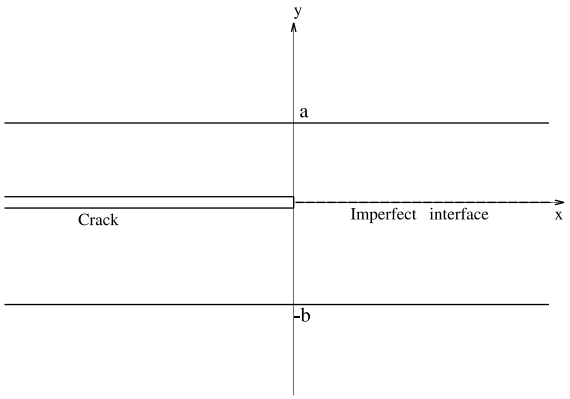

Fig. 3. Strip with semi-infinite crack along the imperfect interface.

$$\mu_+ \frac{\partial u}{\partial y}\bigg|_{y=+0} = \mu_- \frac{\partial u}{\partial y}\bigg|_{y=-0} = \mu[u]_{x=-0}^{x=+0}, \quad x > 0, \tag{3.3}$$

$$\mu_+ \frac{\partial u}{\partial y}\bigg|_{y=+0} = \mu_- \frac{\partial u}{\partial y}\bigg|_{y=-0} = p(x), \quad x < 0, \tag{3.4}$$

where μ_+, μ_- denote the shear moduli of the elastic material occupying the upper and lower parts of the strip; $p(x)$ characterises the shear load applied to the crack faces; μ is the stiffness coefficient of the interface layer (see Section 2). We seek the solution with the finite energy

$$\mathscr{E}(u) = \int_{\mathbb{R}\times[-b,a]} |\nabla u|^2 \,\mathrm{d}x\,\mathrm{d}y. \tag{3.5}$$

3.2. Exact solution of the problem

First, consider an auxiliary problem for the upper part of the strip $(0 < y < a)$

$$\nabla^2 u(x,y) = 0, \quad |x| < \infty, \quad 0 < y < a, \tag{3.6}$$

$$u(x,a) = 0, \quad |x| < \infty, \tag{3.7}$$

$$\mu_+ \frac{\partial u}{\partial y}\bigg|_{y=+0} = \mathscr{P}(x), \quad |x| < \infty, \tag{3.8}$$

where for negative x the function $\mathscr{P}$ is given by $\mathscr{P}(x) = p(x)$, and for $x > 0$ this function is proportional to the displacement jump $\mathscr{P}(x) = \mu\chi(x)$,

$$\chi(x) = u(x,+0) - u(x,-0).$$

Applying the Fourier transform with respect to x

$$u_\alpha(y) = \int_{-\infty}^{+\infty} u(x,y)\,\mathrm{e}^{\mathrm{i}\alpha x}\,\mathrm{d}x \tag{3.9}$$

we obtain the boundary value problem for an ordinary differential equation, which has the following solution

$$u_\alpha(y) = -\frac{\mathscr{P}_\alpha \sinh\alpha(a-y)}{\mu_+ \alpha\cosh(\alpha a)}, \quad 0 < y < a. \tag{3.10}$$

Here and in the text below the subscript index α denotes the Fourier transform. In a similar way, we formulate the auxiliary problem for the lower part of the strip $(-b < y < 0)$ and find

$$u_\alpha(y) = \frac{\mathscr{P}_\alpha \sinh\alpha(b+y)}{\mu_- \alpha\cosh(\alpha b)}, \quad -b < y < 0. \tag{3.11}$$

Thus,

$$\chi_\alpha = u_\alpha(+0) - u_\alpha(-0) = -\frac{\mathscr{P}_\alpha}{\alpha}\left(\frac{\tanh\alpha a}{\mu_+} + \frac{\tanh\alpha b}{\mu_-}\right). \tag{3.12}$$

Note that the displacement jump function $\chi(x)$ is unknown everywhere along the real axis.

We introduce a function ψ with supp $\psi(x) \in (-\infty, 0)$, and rewrite the conditions (3.3) and (3.4) in the form

$$\mu_\pm \frac{\partial u}{\partial y}(x, \pm 0) = \mu\chi(x) + \psi(x), \quad |x| < \infty. \tag{3.13}$$

After taking the Fourier transform with respect to x

$$\mathscr{P}_\alpha = \mu\chi_\alpha + \Phi^-(\alpha), \tag{3.14}$$

where

$$\Phi^-(\alpha) = \psi_\alpha = \int_{-\infty}^{0} \psi(\xi)\,\mathrm{e}^{\mathrm{i}\alpha\xi}\,\mathrm{d}\xi. \tag{3.15}$$

After χ_α in Eq. (3.14) has been replaced by Eq. (3.12) we arrive at the Wiener–Hopf functional equation

$$\Phi^-(\alpha) = G(\alpha)[\mu\Phi^+(\alpha) + P^-(\alpha)], \quad -\infty < \alpha < +\infty. \tag{3.16}$$

Here,

$$\Phi^+(\alpha) = \int_0^\infty \chi(\xi)\,\mathrm{e}^{\mathrm{i}\alpha\xi}\,\mathrm{d}\xi, \quad P^-(\alpha) = \int_{-\infty}^{0} p(\xi)\,\mathrm{e}^{\mathrm{i}\alpha\xi}\,\mathrm{d}\xi \tag{3.17}$$

and

$$G(\alpha) = 1 + \frac{\mu}{\alpha}\left(\frac{\tanh\alpha a}{\mu_+} + \frac{\tanh\alpha b}{\mu_-}\right). \tag{3.18}$$

It is emphasised that the function $\Phi^+(\alpha)$ is analytic in the upper half-plane $\mathbb{C}^+ = \{\alpha : \mathrm{Im}\,\alpha > 0\}$ and the functions $P^-(\alpha)$, $\Phi^-(\alpha)$ are analytic in the lower half-plane $\mathbb{C}^- = \{\alpha : \mathrm{Im}\,\alpha < 0\}$. The boundary values of the unknown functions Φ^+ and Φ^- satisfy the Eq. (3.16) on the real axis.

The function $G(\alpha)$ is even and has zero increment of arg $G(\alpha)$ along the real axis. It allows for the following factorisation

$$G(\beta) = \frac{X^+(\beta)}{X^-(\beta)}, \quad \beta \in (-\infty, +\infty) \tag{3.19}$$

where for real β, $X^\pm(\beta) = X(\beta \pm \mathrm{i}0)$ and

$$X(\alpha) = \exp\left\{\frac{1}{2\pi\mathrm{i}}\int_{-\infty}^{+\infty} \ln G(\beta)\frac{\mathrm{d}\beta}{\beta-\alpha}\right\} = \exp\left\{\frac{\alpha}{\pi\mathrm{i}}\int_0^{+\infty} \ln G(\beta)\frac{\mathrm{d}\beta}{\beta^2-\alpha^2}\right\}, \quad \alpha \in \mathbb{C}\setminus\mathbb{R}^1. \tag{3.20}$$

Note that the function $G(\alpha)$ given by Eq. (3.18) is bounded at the origin and tends to 1 as $\alpha \to \pm\infty$. First we substitute Eq. (3.19) into Eq. (3.16) and then represent $X^+(\alpha)P^-(\alpha)$ as

$$X^+(\alpha)P^-(\alpha) = \Psi^+(\alpha) - \Psi^-(\alpha), \quad \alpha \in \mathbb{R}^1,$$

where $\Psi^\pm(\alpha)$ are the limit values of the function

$$\Psi(\alpha) = \frac{1}{2\pi \mathrm{i}} \int_{-\infty}^{+\infty} \frac{X^+(\beta)P^-(\beta)}{\beta - \alpha}\, \mathrm{d}\beta. \tag{3.21}$$

It yields the following form of Eq. (3.16)

$$X^-(\alpha)\Phi^-(\alpha) + \Psi^-(\alpha) = \mu X^+(\alpha)\Phi^+(\alpha) + \Psi^+(\alpha) \tag{3.22}$$

that is valid in the whole complex plane due to the continuation principle. We are looking for a solution (χ, ψ) integrable in the vicinity of the crack tip. According to Abelian type theorems (see Noble, 1988) the functions $\Phi^\pm(\alpha)$ vanish as $\alpha \to \infty$, $\alpha \in \mathbb{C}^\pm$. Also, $X^\pm(\alpha)$ are bounded and $\Psi^\pm(\alpha)$ vanish as $\alpha \to \infty$, $\alpha \in \mathbb{C}^\pm$. Due to Liouville's theorem, the entire function corresponding to Eq. (3.22) is identically zero. It follows that the functions $\Phi^\pm(\alpha)$ can be represented in the form

$$\Phi^-(\alpha) = -\frac{\Psi^-(\alpha)}{X^-(\alpha)}, \quad \alpha \in \mathbb{C}^-, \quad \Phi^+(\alpha) = -\frac{\Psi^+(\alpha)}{\mu X^+(\alpha)}, \quad \alpha \in \mathbb{C}^+. \tag{3.23}$$

As an example, consider the case when the right-hand side $p(x)$ in Eq. (3.4) can be approximated by

$$p(x) \sim \sum_{k=1}^{N} d_k\, \mathrm{e}^{\alpha_k x}, \quad \alpha_k > 0, \quad x < 0 \tag{3.24}$$

where d_k, α_k are constant coefficients: $\alpha_1 < \alpha_2 < \cdots < \alpha_N$. Then, the function $P^-(\alpha)$ can be written explicitly

$$P^-(\alpha) = \sum_{k=1}^{N} \frac{d_k}{\mathrm{i}\alpha + \alpha_k}.$$

After we have evaluated the Cauchy integrals (3.21) the solution of the Wiener–Hopf problem in the case (3.24) is reduced to the form

$$\Phi^-(\alpha) = -\frac{\mathrm{i}}{X^-(\alpha)} \sum_{k=1}^{N} \frac{d_k X_k}{\alpha - \mathrm{i}\alpha_k}, \quad \alpha \in \mathbb{C}^-, \tag{3.25}$$

$$\Phi^+(\alpha) = \frac{\mathrm{i}}{\mu} \sum_{k=1}^{N} \frac{d_k}{\alpha - \mathrm{i}\alpha_k} \left[1 - \frac{X_k}{X^+(\alpha)}\right], \quad \alpha \in \mathbb{C}^+, \tag{3.26}$$

where

$$X_k = X^+(\mathrm{i}\alpha_k) = \exp\left\{\frac{\alpha_k}{\pi} \int_0^\infty \ln G(\beta) \frac{\mathrm{d}\beta}{\beta^2 + \alpha_k^2}\right\},$$

$$\mathrm{Im} X_k = 0, \quad k = 1, 2, \ldots, N.$$

After applying the inverse Fourier transform

$$\psi(x) = \frac{1}{2\pi} \int_{-\infty}^{+\infty} \Phi^-(\alpha)\, \mathrm{e}^{-\mathrm{i}\alpha x}\, \mathrm{d}\alpha, \quad x < 0,$$

$$\chi(x)=\frac{1}{2\pi}\int_{-\infty}^{+\infty}\Phi^{+}(\alpha)\,\mathrm{e}^{-\mathrm{i}\alpha x}\,\mathrm{d}\alpha,\quad x>0. \tag{3.27}$$

Using the substitution (3.25) and the analytic continuation $X^{-}(\alpha)$ into the upper half-plane $X^{-}(\alpha)=(G(\alpha))^{-1}X^{+}(\alpha)$, $\alpha\in\mathbb{C}^{+}$, we have

$$\psi(x)=\frac{1}{2\pi\mathrm{i}}\sum_{k=1}^{N}d_kX_k\int_{-\infty}^{+\infty}\frac{G(\alpha)\,\mathrm{e}^{-\mathrm{i}\alpha x}}{X^{+}(\alpha)(\alpha-\mathrm{i}\alpha_k)}\,\mathrm{d}\alpha,\quad x<0.$$

Notice that $X^{+}(\alpha)$ is analytic and does not have zeros in $\mathbb{C}^{+}$. The application of the residue theorem yields

$$\psi(x)=\sum_{k=1}^{N}d_k\left\{-\mu X_k\sum_{n=1}^{\infty}\left[\frac{\mathrm{e}^{a_nx}}{a\mu_{+}a_n(a_n-\alpha_k)X^{+}(\mathrm{i}a_n)}+\frac{\mathrm{e}^{b_nx}}{b\mu_{-}b_n(b_n-\alpha_k)X^{+}(\mathrm{i}b_n)}\right]+G(\mathrm{i}\alpha_k)\,\mathrm{e}^{\alpha_kx}\right\},\quad x<0, \tag{3.28}$$

where $a_k=(\pi/2a)(2k-1)$, $b_k=(\pi/2b)(2k-1)$. Here for the sake of simplicity we have assumed that $\alpha_k\neq a_n$ and $\alpha_k\neq b_n$, $k=1,\ldots,N$, for all $n=1,2,\ldots,N$.

In particular, as $x\to-\infty$

$$\psi(x)=\mathrm{O}(\mathrm{e}^{\lambda_0x}),$$

where $\lambda_0=\min\{\pi/2a,\pi/2b,\alpha_1\}$.

It follows from Eqs. (3.13) and (3.28) that for negative x the function $\chi(x)$ has been determined as well

$$\chi(x)=\mu^{-1}\{p(x)-\psi(x)\}.$$

For positive x, we use the second formula in Eq. (3.27) and obtain

$$\chi(x)=\frac{1}{\mu}\sum_{k=1}^{N}d_kX_k\sum_{n=1}^{\infty}\frac{\mathrm{e}^{-\sigma_nx}}{X^{-}(-\mathrm{i}\sigma_n)\mathrm{i}G'(-\mathrm{i}\sigma_n)(\sigma_n+\alpha_k)}$$

where α_k, $\sigma_n>0$, and $-\mathrm{i}\sigma_n$ are the elements of the countable set of roots of $G(\alpha)$ in $\mathbb{C}^{-}$. We note that $\mathrm{Im}\,(X^{\pm}(\pm\mathrm{i}\tau))=0$, $\tau>0$ and $\mathrm{Im}\,(\mathrm{i}G'(-\mathrm{i}\sigma_n))=0$.

3.3. Asymptotics in a neighbourhood of the crack tip

To obtain the asymptotic behaviour of the functions χ, ψ and their derivatives in the vicinity of the origin we consider first their Fourier transforms $\Phi^{\pm}(\alpha)$ (see Eqs. (3.25) and (3.26)) and analyse these functions as $\alpha\to\infty$. To find the asymptotics of the functions $X^{\pm}$, we represent the integral (3.20) in the form

$$\ln X(\alpha)=\frac{\alpha}{\pi\mathrm{i}}\left\{\int_0^{\infty}\left(\ln G(\beta)-\frac{\mu_0}{\beta}\eta(\beta)\right)\frac{\mathrm{d}\beta}{\beta^2-\alpha^2}+\mu_0I(\alpha)\right\}, \tag{3.29}$$

where

$$\mu_0=\mu\left(\frac{1}{\mu_{+}}+\frac{1}{\mu_{-}}\right),\qquad \eta(\beta)=\begin{cases}1, & \beta>1\\ 0, & \beta<1\end{cases},$$

and

$$I(\alpha)=\int_1^{\infty}\frac{\mathrm{d}\beta}{\beta(\beta^2-\alpha^2)}=\frac{-1}{2\alpha^2}[\ln(1+\alpha)+\ln(1-\alpha)].$$

The functions $\ln(1 \pm \alpha)$ are analytic in the complex plane with the cut which joins the branch points $\alpha = -1$, $\alpha = 1$ and passes through infinity. The arguments $\Theta_\pm$ of $\ln(1 \pm \alpha)$ satisfy the condition $-\pi < \Theta_\pm < \pi$. As $\alpha \to \infty$ and $\theta = \arg\ \alpha \in (0, \pi)$, we have $\Theta_+ \to \theta$, $\Theta_- \to \theta - \pi$. If $\theta \in (-\pi, 0)$ and $\alpha \to \infty$ then $\Theta_+ \to \theta$, $\Theta_- \to \theta + \pi$.

Thus, the integral $I(\alpha)$ exhibits different behaviour at infinity in the upper and lower half-planes

$$I(\alpha) \sim \frac{1}{\alpha^2}\left(- \ln(\alpha) \pm \frac{\pi \mathrm{i}}{2}\right), \quad \alpha \to \infty, \alpha \in \mathbb{C}^\pm, \ \arg \alpha \in (-\pi, \pi).$$

Now we can establish the asymptotics of the function $\ln X(\alpha)$ at infinity

$$\ln X(\alpha) = \frac{\mu_0}{\pi \mathrm{i} \alpha} \ln \alpha + \frac{c_1^\pm}{\pi \mathrm{i} \alpha} + \mathrm{O}(\alpha^{-3}), \quad \text{as } \alpha \to \infty, \quad \alpha \in \mathbb{C}^\pm,$$

where

$$c_1^\pm = - \int_0^\infty \left(\ln G(\beta) - \frac{\mu_0}{\beta} \eta(\beta)\right) \mathrm{d}\beta \pm \frac{\mu_0 \pi \mathrm{i}}{2}.$$

The asymptotic expression for $X(\alpha)$ itself takes the form

$$X(\alpha) = 1 - \frac{\mu_0 \ln \alpha}{\pi \mathrm{i} \alpha} + \frac{c_1^\pm}{\pi \mathrm{i} \alpha} - \frac{\mu_0^2}{2\pi^2 \alpha^2} \ln^2 \alpha + c_1^\pm \frac{\mu_0}{\pi^2 \alpha^2} \ln \alpha - \frac{(c_1^\pm)^2}{2\pi^2 \alpha^2} + \mathrm{O}\left(\frac{\ln^3 \alpha}{\alpha^3}\right), \quad \text{as } \alpha \to \infty, \ \alpha \in \mathbb{C}^\pm.$$

It follows from Eqs. (3.25) and (3.26) that the asymptotics for $\Phi^+(\alpha)$ and $\Phi^-(\alpha)$ are given by

$$\Phi^\pm(\alpha) = \sum_{m=0}^{\infty} \alpha^{-(m+1)} \sum_{j=0}^{m} e_{mj}^\pm \ln^j \alpha, \quad \alpha \to \infty, \ \alpha \in \mathbb{C}^\pm, \tag{3.30}$$

where $e_{mj}^\pm$ are constant coefficients. In the text below we shall use several first terms of the expansions (3.30), and restrict ourselves to the coefficients $e_{00}^\pm$, $e_{10}^\pm$ and $e_{11}^\pm$. These quantities are given by

$$e_{00}^- = -\mathrm{i} \sum_{k=1}^{N} d_k X_k, \quad e_{11}^- = \frac{\mu_0}{\pi \mathrm{i}} e_{00}^-,$$

$$e_{10}^- = \sum_{k=1}^{N} d_k X_k \left(\alpha_k + \frac{c_1^-}{\pi}\right)$$

and

$$e_{00}^+ = \frac{\mathrm{i}}{\mu} \sum_{k=1}^{N} d_k + \frac{e_{00}^-}{\mu}, \quad e_{11}^+ = \frac{e_{11}^-}{\mu},$$

$$e_{10}^+ = -\frac{1}{\mu} \sum_{k=1}^{N} d_k \alpha_k + \frac{1}{\mu} \sum_{k=1}^{N} d_k X_k \left(\alpha_k + \frac{c_1^+}{\pi}\right).$$

Hence, as $x \to +0$, the function $\chi(x)$ admits the following asymptotic expansion

$$\chi(x) = \Lambda_{00} + \Lambda_{10} x + \Lambda_{11} x \ln x + \mathrm{O}(x^2 \ln^2 x), \tag{3.31}$$

where

$$\begin{aligned}
\Lambda_{00} &= \frac{1}{\mu}\sum_{k=1}^{N} d_k(1-X_k),\\
\Lambda_{10} &= \frac{1}{\mu}\sum_{k=1}^{N} d_k\left\{\alpha_k + X_k\left[\frac{1}{\pi}r - \alpha_k + \frac{\mu_0}{\pi}(1-\gamma)\right]\right\},\\
\Lambda_{11} &= -\frac{\mu_0}{\pi\mu}\sum_{k=1}^{N} d_k X_k,\\
r &= \int_0^{\infty}\left[\ln G(\beta) - \frac{\mu_0}{\beta}\eta(\beta)\right]\mathrm{d}\beta,
\end{aligned} \tag{3.32}$$

and γ is Euler's constant ($\gamma = 0.57721566\ldots$).

Here we have used the following relations between the coefficients Λ_{mj} and e^{+}_{mj}

$$\Lambda_{00} = -\mathrm{i}e^{+}_{00}, \quad \Lambda_{11} = e^{+}_{11},$$

$$\Lambda_{10} + \Lambda_{11}\left(\frac{\pi\mathrm{i}}{2} + 1 - \gamma\right) = -e^{+}_{10},$$

which can be obtained if we take into account formulae (3.27) and

$$I_k(\alpha) = \int_0^{\infty} \mathrm{e}^{\mathrm{i}\alpha\tau}\tau^k\,\mathrm{d}\tau = \frac{\mathrm{i}\Gamma(k+1)}{\alpha^{k+1}}\mathrm{e}^{(\pi\mathrm{i}/2)k},$$

$$L_k(\alpha) = \int_0^{\infty} \mathrm{e}^{\mathrm{i}\alpha\tau}\tau^k\ln\tau\,\mathrm{d}\tau = \frac{\mathrm{i}\Gamma(k+1)}{\alpha^{k+1}}\mathrm{e}^{(\pi\mathrm{i}/2)k}\left(-\gamma + \sum_{m=1}^{k}\frac{1}{m} + \frac{\pi\mathrm{i}}{2} - \ln\alpha\right), \quad 0 < \arg\alpha < \pi.$$

The last relation follows from formula 4.352(1) (Gradshteyn and Ryzhik, 1980). Alternatively, it can be reduced from the previous relationship in the limit,

$$L_k(\alpha) = \lim_{\beta\to 0}\frac{I_{k+\beta}(\alpha) - I_k(\alpha)}{\beta}.$$

Next, we consider the derivative $\mathrm{d}\chi/\mathrm{d}x$, as $x \to +0$. It has the logarithmic singularity characterised by the following asymptotics

$$\frac{\mathrm{d}}{\mathrm{d}x}\chi(x) \sim \Lambda_{11}\ln x + \mathrm{O}(1), \quad x \to +0. \tag{3.33}$$

The case when $x \to -0$ requires the knowledge of function $\psi(x)$ (see Eq. (3.13)). It has the asymptotic representation

$$\psi(x) \sim M_{00} - M_{10}x - M_{11}x\ln(-x) + \cdots, \quad x \to -0, \tag{3.34}$$

obtained in a similar way to the one used for the function χ when $x \to +0$. Here, the coefficients M_{00}, M_{10} and M_{11} are defined by

$$\begin{aligned}
M_{00} &= \sum_{k=1}^{N} d_k X_k, \quad M_{11} = -\frac{\mu_0}{\pi}M_{00},\\
M_{10} &= \sum_{k=1}^{N} d_k X_k\left[\frac{r}{\pi} - \alpha_k + \frac{\mu_0}{\pi}(1-\gamma)\right].
\end{aligned} \tag{3.35}$$

It follows from Eq. (3.13) that

$$\chi(-0)=\frac{1}{\mu}(p(-0)-\psi(-0))=\frac{1}{\mu}\sum_{k=1}^{N}d_k(1-X_k)=\chi(+0),$$

and therefore, the displacement jump $[u](x)$ is continuous at the crack tip ($x=0$). Moreover, in the neighbourhood of the point $x=0$ the function $\chi(x)$ admits the following expansion

$$\chi(x)=\Lambda_{00}+\Lambda_{10}x+\Lambda_{11}x\ln|x|+\cdots,\quad x\to 0. \tag{3.36}$$

For the derivative $\psi'(x)$, the expression (3.34) yields

$$\psi'(x)=-M_{11}\ln(-x)+\mathrm{O}(1),\quad x\to -0. \tag{3.37}$$

From Eq. (3.36) we deduce

$$\chi'(x)=\Lambda_{11}\ln|x|+\mathrm{O}(1),\quad x\to 0. \tag{3.38}$$

Since the displacement jump $\chi(x)$ is continuous at $x=0$, and the function $\psi(x)$ is discontinuous,

$$\psi(+0)=0,\quad \psi(-0)=M_{00}\neq 0,$$

we conclude (see Eq. (3.13)) that the traction

$$\sigma_{zy}(x,0)=\mu_+\frac{\partial u}{\partial y}(x,+0)=\mu_-\frac{\partial u}{\partial y}(x,-0)$$

is bounded but discontinuous at the crack tip,

$$[\sigma_{zy}(x,0)]_{x=-0}^{x=+0}=-\psi(-0)=-M_{00}.$$

The formula (3.38) shows that the stress component $\sigma_{zx}(x,0)$ has the logarithmic singularity at $x=0$.

4. The Neumann problem for a strip with a semi-infinite crack along the imperfect interface

The formulation is similar to Section 3, with Dirichlet boundary conditions on the upper and lower parts of the strip being replaced by the homogeneous Neumann data (see Fig. 3). The unknown function $u(x,y)$ satisfies the Eq. (3.1) and the contact conditions (3.3) and (3.4). Instead of Eq. (3.2), we assume that

$$\frac{\partial u}{\partial y}(x,a)=\frac{\partial u}{\partial y}(x,-b)=0,\quad |x|<\infty. \tag{4.1}$$

We seek the solution in the class of functions with the finite energy integral (3.5) and with the following behaviour at infinity

$$|u(x,y)|<C_1,\quad \text{as } x\to-\infty,$$

and

$$|u(x,y)|<C_2\mathrm{e}^{-\delta x},\quad \text{as } x\to+\infty,$$

uniformly with respect to $-b<y<a$, where C_1, C_2 and δ are positive constants. To specify the solution uniquely, we impose the following orthogonality condition

$$\int_{-\infty}^{\infty}\frac{\partial u}{\partial y}(x,\pm 0)\,\mathrm{d}x=0. \tag{4.2}$$

4.1. Analysis of the Wiener–Hopf functional equation

The choice of the above function class ensures the existence of the Fourier transform $u_\alpha(y)$ defined by Eq. (3.9) in the strip $-\delta < \operatorname{Im}\alpha < 0$.

Following the same pattern as in Section 3 we consider two auxiliary formulations in the upper and the lower parts of the strip and obtain the following functional equation of the Wiener–Hopf type

$$\Phi^-(\alpha) = G(\alpha)[\mu\Phi^+(\alpha) + P^-(\alpha)], \quad \alpha \in \Gamma, \quad \Gamma = \{\alpha : \operatorname{Im}\alpha = -\delta_0 \in (-\delta, 0)\},$$

where

$$G(\alpha) = 1 + \frac{\mu}{\alpha}\left(\frac{\coth \alpha a}{\mu_+} + \frac{\coth \alpha b}{\mu_-}\right). \tag{4.3}$$

Here the constants μ, μ_+ and μ_- are the same as in Section 3. The functions $\Phi^\pm(\alpha)$ and $P^-(\alpha)$ are defined by Eqs. (3.15) and (3.17): $\Phi^+(\alpha)$ is analytic in the domain D^+, and $\Phi^-(\alpha)$, $P^-(\alpha)$ are analytic in D^-, where

$$D^+ = \{\alpha : \operatorname{Im}\alpha > -\delta_0\}, \quad D^- = \{\alpha : \operatorname{Im}\alpha < -\delta_0\}.$$

Here, the quantity $\delta_0 > 0$ has been chosen in such a way that the strip $\{-\delta_0 < \operatorname{Im}\alpha < 0\}$ does not include any roots of the function $G(\alpha)$.

The function $G(\alpha)$ has the second-order pole at the point $\alpha = 0 \in D^+$. In order to compute the increment of $\Theta = \arg G(\alpha)$, we deform the contour Γ to the shape shown in Fig. 4. The positive direction of contour Γ is chosen in such a way that the domain D^+ is on the left. We consider the following points on the deformed contour

$$A_\infty^\pm: \quad \alpha = \pm\infty - \mathrm{i}0,$$

$$A_0^\pm: \quad \alpha = \pm\delta_0 - \mathrm{i}0,$$

$$A_1^\pm: \quad \alpha = \frac{\delta_0}{\sqrt{2}}(\pm 1 - \mathrm{i}),$$

$$A: \quad \alpha = -\delta_0\mathrm{i}.$$

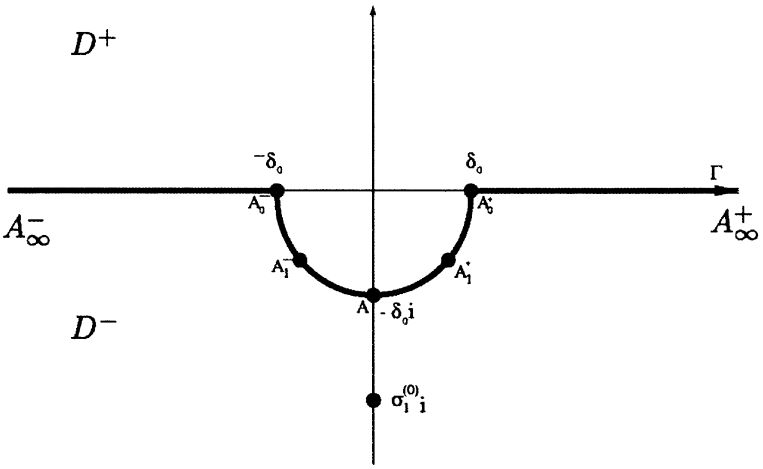

Fig. 4. The contour Γ.

At the starting point A_∞^-, the function $G(\alpha)=1$. At this point, we set $\Theta=2\pi$. As α runs from A_∞^- to A_0^-, the argument Θ of $G(\alpha)$ does not change. As the radius δ_0 of the circle in Fig. 4 tends to zero, the value $G(A_0^-)$ behaves as $G(A_0^-)\sim\delta^{-2}\mu_1$, where $\mu_1=\mu(1/a\mu_+ + 1/b\mu_-)$. As α travels from A_0^- to A_1^-, the argument of the principal part of G changes from 2π to $3\pi/2$, and for small δ_0, the real and imaginary parts of $G(A_1^-)$ have the following leading terms

$$\operatorname{Re} G(A_1^-)\sim 1,\quad \operatorname{Im} G(A_1^-)\sim -\frac{\mu_1 \mathrm{i}}{\delta_0^2}.$$

Next, the argument Θ reduces further down to π at the point A, and $G(A)\sim -\mu_1/\delta_0^2$ as $\delta_0\to 0$. In a similar way it can be shown that, as $\delta_0\to 0$,

$$\begin{aligned}
&\operatorname{Re} G(A_1^+)\sim 1,\quad \operatorname{Im} G(A_1^+)\sim \delta_0^{-2}\mu_1,\quad \Theta|_{\alpha=A_1^+}\sim\frac{\pi}{2},\\
&G(A_0^+)\sim\delta_0^{-2}\mu_1,\quad \Theta|_{\alpha=A_0^+}=0,\\
&G(A_\infty^+)=1,\quad \Theta|_{\alpha=A_\infty^+}=0.
\end{aligned}$$

Thus, we have shown that $\arg\ G(\alpha)$ changes from 2π down to 0 as α travels from A_∞^- to A_∞^+ along the contour Γ (see Fig. 5). According to the definition of the index of the Riemann boundary value problem (see Gakhov, 1966), it is equal to

$$\kappa=-\mathrm{ind}_\Gamma G(\alpha)=-\frac{1}{2\pi}[\arg G(\alpha)]_\Gamma=1.$$

It shows that the solution of the Riemann boundary value problem (4.3) will be specified up to an arbitrary constant. We take into account that

$$\left[\arg\frac{\alpha-\mathrm{i}}{\alpha+\mathrm{i}}\right]_\Gamma=2\pi,$$

and we introduce the quantity $(\alpha+1)^{-1}(\alpha-\mathrm{i})G(\alpha)$ which satisfies the condition

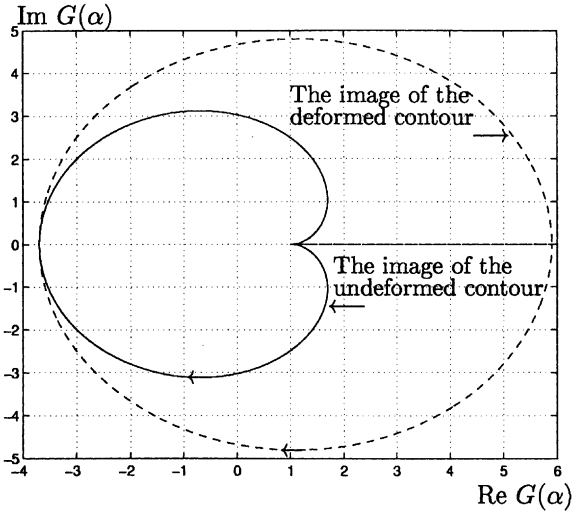

Fig. 5. The parametrically defined function $G(\alpha)$, with α travelling along the contour Γ.

$$\left[\arg\left(\frac{\alpha-\mathrm{i}}{\alpha+\mathrm{i}}G(\alpha)\right)\right]_{\Gamma}=0,$$

and can be factorised as follows

$$\frac{t-\mathrm{i}}{t+\mathrm{i}}G(t)=\frac{X^{+}(t)}{X^{-}(t)},\quad t\in\Gamma, \tag{4.4}$$

where

$$X^{\pm}(\alpha)=\exp\left\{\frac{1}{2\pi\mathrm{i}}\int_{\Gamma}\ln\left(\frac{t-\mathrm{i}}{t+\mathrm{i}}G(t)\right)\frac{\mathrm{d}t}{t-\alpha}\right\},\quad \alpha\in D^{\pm}.$$

It follows from Eqs. (4.3) and (4.4) that

$$\Phi^{-}(t)(t-\mathrm{i})X^{-}(t)+\Psi^{-}(t)=\mu\Phi^{+}(t)(t+\mathrm{i})X^{+}(t)+\Psi^{+}(t),\quad t\in\Gamma, \tag{4.5}$$

where $\Psi^{\pm}(t)$ are the one-sided limits of the function

$$\Psi(\alpha)=\frac{1}{2\pi\mathrm{i}}\int_{\Gamma}\frac{(t+\mathrm{i})X^{+}(t)P^{-}(t)}{t-\alpha}\,\mathrm{d}t,\quad \alpha\in\mathbb{C}\setminus\Gamma.$$

Compared to Eq. (3.22), in Eq. (4.5) we have additional factors $t\mp\mathrm{i}$ in front of $X^{\pm}$. Consequently the entire function is bounded at infinity and is equal to a constant C everywhere in the complex plane. Thus, the functions $\Phi^{\pm}$ are given by

$$\Phi^{+}(\alpha)=\frac{C-\Psi^{+}(\alpha)}{\mu(\alpha+\mathrm{i})X^{+}(\alpha)},\quad \alpha\in D^{+},$$

$$\Phi^{-}(\alpha)=\frac{C-\Psi^{-}(\alpha)}{(\alpha-\mathrm{i})X^{-}(\alpha)},\quad \alpha\in D^{-}.$$

The constant C is determined by the condition (4.2) that can be rewritten in the form

$$\mu\Phi^{+}(0)+P^{-}(0)=0,$$

where $P^{-}(0)=\int_{-\infty}^{0}p(x)\,\mathrm{d}x$ is finite since the external load $p(x)$ is integrable on $(-\infty,0)$. We have

$$C=\Psi^{+}(0)-\mathrm{i}X^{+}(0)P^{-}(0).$$

As in the previous section, we consider the particular case when the applied load is represented by Eq. (3.24). Then the solution of the Wiener–Hopf problem (4.3) is given by

$$\Phi^{+}(\alpha)=\frac{\mathrm{i}}{\mu}\sum_{k=1}^{N}\frac{1}{\alpha-\mathrm{i}\alpha_k}\left\{d_k-\frac{\alpha d_k^{0}}{(\alpha+\mathrm{i})X^{+}(\alpha)\alpha_k}\right\},$$

$$\Phi^{-}(\alpha)=\frac{-\mathrm{i}\alpha}{(\alpha-\mathrm{i})X^{-}(\alpha)}\sum_{k=1}^{N}\frac{d_k^{0}}{\alpha_k(\alpha-\mathrm{i}\alpha_k)}, \tag{4.6}$$

where $d_k^{0}=d_k(\alpha_k+1)X_k$, $X_k=X^{+}(\mathrm{i}\alpha_k)$. Analysing asymptotics of $\Phi^{\pm}(\alpha)$ as $\alpha\to\infty$, $\alpha\in\mathbb{C}^{\pm}$ we obtain the representation of the function $\chi(x)$ as $x\to 0$. The asymptotic formula is the same as in the previous section (see Eq. (3.36)) with the different coefficients Λ_{00}, Λ_{10}, Λ_{11}. We confine ourselves to give the principal coefficient

$$\Lambda_{00}=\frac{1}{\mu}\sum_{k=1}^{N}d_k\left(1-X_k\frac{\alpha_k+1}{\alpha_k}\right). \tag{4.7}$$

As in the previous section, it is observed that the shear stress $\sigma_{zx}(x,0)$ has the logarithmic singularity at $x=0$ and $\sigma_{zy}(x,0)$ possesses a discontinuity of the first kind.

4.2. The displacement jump

The functions $\psi(x)$ and $\chi(x)$ are determined as the inverse Fourier transforms

$$\psi(x)=\begin{cases}\frac{1}{2\pi}\int_\Gamma \Phi^-(\alpha)\,\mathrm{e}^{-\mathrm{i}\alpha x}\,\mathrm{d}\alpha, & x<0\\ 0, & x>0\end{cases} \tag{4.8}$$

and

$$\chi(x)=\begin{cases}\frac{-1}{\mu}(\psi(x)-p(x)), & x<0\\ \frac{1}{2\pi}\int_\Gamma \Phi^+(\alpha)\,\mathrm{e}^{-\mathrm{i}\alpha x}\,\mathrm{d}\alpha, & x>0.\end{cases} \tag{4.9}$$

Substituting Φ^- from Eq. (4.6) into Eq. (4.8) we continue analytically $X^-(\alpha)$ into D^+ (see Eq. (4.4)) and observe that the integrand has a simple pole at the point $\alpha=0$. Using the residue theorem we obtain

$$\psi(x)=A+\sum_{k=1}^{N} d_k G(\mathrm{i}\alpha_k)\,\mathrm{e}^{\alpha_k x}-\sum_{n=1}^{\infty}\frac{\mu}{\pi n}\left(\frac{1}{\mu_+}\mathscr{F}(a_n^{(0)},x)+\frac{1}{\mu_-}\mathscr{F}(b_n^{(0)},x)\right), \quad x<0, \tag{4.10}$$

where

$$A=\frac{\mu_1}{X^+(0)}\sum_{k=1}^{N}\frac{d_k^0}{\alpha_k^2},$$

and

$$\mathscr{F}(c_n,x)=\frac{\mathrm{e}^{c_n x}}{(c_n+1)X^+(\mathrm{i}c_n)}\sum_{k=1}^{N}\frac{c_n d_k^0}{(c_n-\alpha_k)\alpha_k}.$$

The positive coefficients α_k are the same as in the previous section (see formula (3.24)), and the constants $a_n^{(0)}$, $b_n^{(0)}$ are given by

$$a_n^{(0)}=\frac{\pi n}{a}, \quad b_n^{(0)}=\frac{\pi n}{b}.$$

In contrast to the Dirichlet problem studied in the previous section, the functions $\psi(x)$ and $\chi(x)$ do not vanish as $x\to-\infty$:

$$\psi(x)=A+\mathrm{O}(\mathrm{e}^{\lambda_1 x}),$$

$$\chi(x)=-\frac{1}{\mu}A+\mathrm{O}(\mathrm{e}^{\lambda_1 x}),$$

where

$$\lambda_1=\min\{\alpha_1,\pi/a,\pi/b\}.$$

For positive x, the function ψ vanishes (see Eq. (4.8)), and χ is determined by

$$\chi(x)=\frac{-\mathrm{i}}{\mu}\sum_{n=1}^{\infty}\frac{\mathrm{e}^{-\sigma_n^{(0)}x}}{X^-(-\mathrm{i}\sigma_n^{(0)})(\sigma_n^{(0)}+1)G'(-\mathrm{i}\sigma_n^{(0)})}\sum_{k=1}^{N}\frac{d_k^0\sigma_n^{(0)}}{(\sigma_n^{(0)}+\alpha_k)\alpha_k}.$$

Here $-\mathrm{i}\sigma_n^{(0)}$ denotes the roots of the function $G(\alpha)$ (see Eq. (4.3)) in D^-. As $x\to+\infty$, $\chi(x)$ vanishes exponentially:

$$\chi(x) = \mathrm{O}(\mathrm{e}^{-\sigma_1^{(0)}x}), \quad x \to +\infty.$$

We note that $\sigma_1^{(0)}$ determines the range of change of radius of the semi-circle on the contour Γ (see Fig. 4): $0 < \delta_0 < \sigma_1^{(0)}$.

5. Infinite plane with a semi-infinite delamination crack

Consider an infinite two-phase plane with the line of imperfect interface along the x-axis. A semi-infinite delamination crack is introduced on (x,y):$y = 0$, $x < 0$ (see Fig. 3). The problem of anti-plane shear is formulated as follows. The displacement function u satisfies the Laplace equation

$$\nabla^2 u(x,y) = 0, \quad \text{in } \mathbb{R}^2 \setminus \{y = 0\},$$

the contact conditions

$$\mu_+ \frac{\partial u}{\partial y}\bigg|_{y=+0} = \mu_- \frac{\partial u}{\partial y}\bigg|_{y=-0},$$
$$\mu_\pm \frac{\partial u}{\partial y}\bigg|_{y=\pm 0} = \mu[u], \quad \text{for } x > 0,$$

and the following boundary condition on the crack faces

$$\mu_\pm \frac{\partial u}{\partial y}\bigg|_{y=\pm 0} = p(x), \quad x < 0.$$

Here, the right-hand side $p(x)$ is chosen in such a way that the problem has the solution with the finite energy integral (3.5).

Taking the Fourier transforms with respect to x (see Eq. (3.9)) and following the same pattern as in Section 3 we obtain the functional equation of the Wiener–Hopf type on the real axis:

$$\Phi^-(\alpha) = G(\alpha)(\mu\Phi^+(\alpha) + P^-(\alpha)), \quad \alpha \in (-\infty, +\infty), \tag{5.1}$$

where $G(\alpha) = 1 + (\mu_0/|\alpha|)$. We note that the function G is real and positive on the real axis, and can be factorised in the form

$$G(\alpha) = \frac{X^+(\alpha)}{X^-(\alpha)},$$

where the functions $X^\pm(\alpha)$ are the limiting values of

$$X(\alpha) = \exp\left\{\frac{1}{2\pi\mathrm{i}} \int_{-\infty}^{+\infty} \ln\left(1 + \frac{\mu_0}{|\beta|}\right) \frac{\mathrm{d}\beta}{\beta - \alpha}\right\}. \tag{5.2}$$

As in Section 3, the relationship (5.1) is reduced to the form (3.22), where the functions $X^\pm$ are defined by Eq. (5.2). The solution of Eq. (5.1) is given by Eq. (3.23). To obtain the behaviour of the displacement in a neighbourhood of the crack tip and at infinity, we analyse the solution $\Phi^+(\alpha)$, $\Phi^-(\alpha)$ as $\alpha \to \infty$ or $\alpha \to 0$.

In the vicinity of the crack tip, the behaviour of the displacement is similar to the one discussed in Sections 3 and 4 (see Eq. (3.31)). The qualitative difference between these two cases is observed when $x \to -\infty$. In contrast with Sections 3 and 4, the functions $X^\pm$ are characterised by the following asymptotics

$$X^+(\alpha) = (-\mathrm{i}\alpha)^{-(1/2)}\left(\mu_0^{1/2} + \mathrm{O}(1)\right) \quad \text{as } \alpha \to 0, \ \ \alpha \in \mathbb{C}^+,$$
$$X^-(\alpha) = (\mathrm{i}\alpha)^{1/2}\left(\mu_0^{-1/2} + \mathrm{O}(1)\right) \quad \text{as } \alpha \to 0, \ \ \alpha \in \mathbb{C}^-. \tag{5.3}$$

As in the previous two sections, we consider the special case of applied load specified by Eq. (3.24). Then the formulae (3.25) and (3.26) can be used to determine the asymptotics of functions $\Phi^{\pm}(\alpha)$ at the point $\alpha = 0$:

$$\Phi^+(\alpha) \sim B_+, \quad \alpha \to 0, \quad \alpha \in \mathbb{C}^+, \quad \Phi^-(\alpha) \sim (\mathrm{i}\alpha)^{-(1/2)} B_-, \quad \alpha \to 0, \quad \alpha \in \mathbb{C}^-, \tag{5.4}$$

where

$$B_+ = -\frac{1}{\mu}\sum_{k=1}^{N}\frac{d_k}{\alpha_k} \quad \text{and} \quad B_- = \mu_0^{1/2}\sum_{k=1}^{N}\frac{d_k}{\alpha_k}X^+(\mathrm{i}\alpha_k).$$

Using the definition (3.15) and the second asymptotic formula (5.4) we obtain the asymptotic behaviour of $\psi(\xi)$ as $x \to -\infty$

$$\psi(\xi) \sim \frac{B_-}{\sqrt{\pi}}(-x)^{-(1/2)}. \tag{5.5}$$

To derive Eq. (5.5), we have used the Abelian type theorem. Thus, due to Eq. (3.13), the function χ characterising the displacement jump has the square root asymptotics at infinity

$$\chi(x) \sim -\frac{B_-}{\mu\sqrt{\pi}}(-x)^{-(1/2)}, \quad x \to -\infty. \tag{5.6}$$

As $x \to +\infty$, it follows from Eq. (3.26) that the function $\chi(x)$ decays algebraically

$$\chi(x) = \mathrm{O}(x^{-(3/2)}), \quad x \to +\infty.$$

We note that the function χ, specified in the previous sections for a finite strip, decays exponentially as $x \to +\infty$.

6. Plane strain problem for a strip with a finite crack along an imperfect interface

We consider the domain with the same geometry as in Section 3 but with the crack along the imperfect interface being finite (see Fig. 6). Let the displacement vector $\boldsymbol{u} = (u, v)$ satisfy the homogeneous equilibrium equations

$$\nabla^2\boldsymbol{u} + \frac{1}{1-2\nu_\pm}\nabla\nabla\cdot\boldsymbol{u} = 0 \quad \text{in } \mathscr{H},$$

where $\mathscr{H} = \{(x,y)\colon x \in \mathbb{R},\ y \in (-b,a)\setminus\{0\}\}$ and the subscript "+" is allocated for the upper layer $0 < y < a$, and the subscript "−" corresponds to the lower layer $-b < y < 0$; $\nu_\pm$ denotes the Poisson ratio of the material of the upper and lower layers. Homogeneous traction conditions are posed on the upper and lower parts of the boundary

$$\tau_{xy} = \sigma_y = 0 \quad \text{on } \mathscr{B}^+ \quad \text{and} \quad \mathscr{B}^-,$$

where $\mathscr{B}^+ = \{(x,y)\colon x \in \mathbb{R},\ y = a\}$, $\mathscr{B}^- = \{(x,y)\colon x \in \mathbb{R},\ y = -b\}$. The traction conditions are specified on the crack faces

$$\tau_{xy} = f_1(x), \qquad \sigma_y = f_2(x) \quad \text{as } |x| < c, \quad y = 0, \tag{6.1}$$

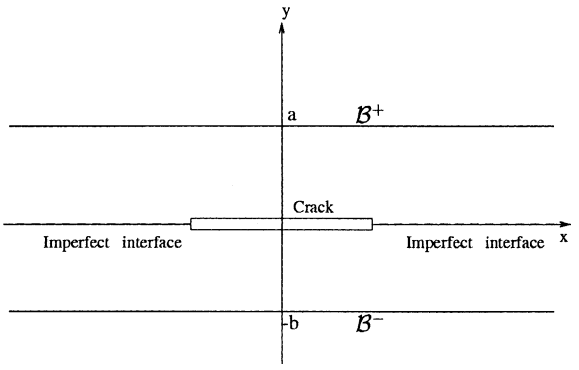

Fig. 6. Strip with finite crack along the imperfect interface.

and the interface conditions are given outside the crack by

$$\begin{aligned} \tau_{xy}(x,0) &= \alpha_{11}[u] + \alpha_{12}[v], \\ \sigma_y(x,0) &= \alpha_{12}[u] + \alpha_{22}[v] \\ [\sigma_y] = [\tau_{xy}] &= 0 \quad \text{as } |x| > c, \quad y = 0. \end{aligned} \tag{6.2}$$

Here

$$[g] = g|_{y=+0} - g|_{y=-0}.$$

We seek the solution with finite elastic energy, and assume that the displacement field decays at infinity.

6.1. The system of integral equations

We introduce the following notations for displacement jump components

$$\chi_1(x) = [u](x), \quad \chi_2(x) = [v](x), \quad |x| < \infty, \tag{6.3}$$

and for traction components

$$\sigma(x) = \sigma_y(x,0), \quad \tau(x) = \tau_{xy}(x,0), \quad |x| < \infty.$$

Let U denote the Airy function. Then the stress components and derivatives of displacements are given by

$$\sigma_y = \frac{\partial^2 U}{\partial x^2}, \quad \sigma_x = \frac{\partial^2 U}{\partial y^2}, \quad \tau_{xy} = -\frac{\partial^2 U}{\partial x \partial y},$$

and

$$\begin{aligned} 2\mu_\pm \frac{\partial u}{\partial x} &= (1 - \nu_\pm)\frac{\partial^2 U}{\partial y^2} - \nu_\pm \frac{\partial^2 U}{\partial x^2}, \\ 2\mu_\pm \frac{\partial v}{\partial y} &= (1 - \nu_\pm)\frac{\partial^2 U}{\partial x^2} - \nu_\pm \frac{\partial^2 U}{\partial y^2}, \\ \mu_\pm \left(\frac{\partial u}{\partial y} + \frac{\partial v}{\partial x} \right) &= -\frac{\partial^2 U}{\partial x \partial y}, \end{aligned} \tag{6.4}$$

where $\mu_\pm$ denotes the shear moduli of the material in the upper and lower parts of the composite strip.

First, we consider the upper part of the strip ($0 < y < a$). The function U satisfies the boundary value problem

$$\Delta^2 U(x,y) = 0 \quad |x| < \infty, \quad 0 < y < a,$$
$$\frac{\partial^2 U}{\partial x^2} = \frac{\partial^2 U}{\partial x\,\partial y} = 0, \quad |x| < \infty, \quad y = a,$$
$$\frac{\partial^2 U}{\partial x^2} = \sigma(x), \quad -\frac{\partial^2 U}{\partial x\,\partial y} = \tau(x), \quad |x| < \infty, \quad y = 0.$$

Taking the Fourier transform with respect to x

$$U_\alpha(y) = \int_{-\infty}^{+\infty} U(x,y)\mathrm{e}^{\mathrm{i}\alpha x}\,\mathrm{d}x,$$

we obtain

$$U_\alpha^{(IV)}(y) - 2\alpha^2 U_\alpha''(y) + \alpha^4 U_\alpha(y) = 0, \quad 0 < y < a, \tag{6.5}$$

$$U_\alpha(a) = U_\alpha'(a) = 0, \tag{6.6}$$

$$-\alpha^2 U_\alpha(0) = \sigma_\alpha, \quad \mathrm{i}\alpha U_\alpha'(0) = \tau_\alpha, \tag{6.7}$$

where σ_α, τ_α denote the Fourier transforms of tractions. The solution of the system (6.5)–(6.7) has the form

$$U_\alpha(y) = C_1\cosh(a-y)\alpha + C_2\sinh(a-y)\alpha + C_3(a-y)\cosh(a-y)\alpha + C_4(a-y)\sinh(a-y)\alpha, \tag{6.8}$$

where the constants C_1, C_2, C_3, C_4 are given by

$$C_1 = 0,$$
$$C_2 = \frac{a\sinh(\alpha a)}{\mathrm{i}\alpha d(\alpha a)}\tau_\alpha - \frac{\sinh(\alpha a) + \alpha a\cosh(\alpha a)}{\alpha^2 d(\alpha a)}\sigma_\alpha,$$
$$C_3 = -\alpha C_2,$$
$$C_4 = -\frac{a\sinh(\alpha a)}{d(\alpha a)}\sigma_\alpha - \frac{\sinh(\alpha a) - \alpha a\cosh(\alpha a)}{\mathrm{i}\alpha d(\alpha a)}\tau_\alpha,$$

and $d(\beta) = \sinh^2\beta - \beta^2$.

We need the displacement components on the upper boundary of the interface. Relationships (6.4) and (6.8) yield the following expressions for the Fourier transforms

$$-2\mathrm{i}\alpha\mu_+ u_\alpha(+0) = \frac{(1-2\nu_+)\sinh^2(\alpha a) + \alpha^2 a^2}{d(\alpha a)}\sigma_\alpha + \frac{2(1-\nu_+)\tau_\alpha}{\mathrm{i}d(\alpha a)}(\alpha a - \sinh(\alpha a)\cosh(\alpha a)),$$

$$2\alpha\mu_+ v_\alpha(+0) = \frac{(1-2\nu_+)\sinh^2(\alpha a) + \alpha^2 a^2}{\mathrm{i}d(\alpha a)}\tau_\alpha - \frac{2(1-\nu_+)\sigma_\alpha}{d(\alpha a)}(\alpha a + \sinh(\alpha a)\cosh(\alpha a)). \tag{6.9}$$

In general, one can add arbitrary rigid-body translations and rotations. Here, we have assumed that these terms are equal to zero, which is consistent with the assumption of decay at infinity introduced at the beginning of the section.

In a similar way, one can write the boundary value problem for U_α in the lower part of the strip and obtain the Fourier transforms of the displacement components $u_\alpha(-0)$ and $v_\alpha(-0)$ which have the form (6.9) where a should be replaced by $-b$ and μ_+, ν_+ should be replaced by μ_-, ν_-. Thus, the Fourier transforms of the functions χ_1, χ_2 (see Eq. (6.3)) are

$$\begin{aligned}
&\mathrm{i}\alpha\chi_{1\alpha} = -g(\alpha)\sigma_\alpha + \mathrm{i}h_-(\alpha)\tau_\alpha,\\
&\mathrm{i}\alpha\chi_{2\alpha} = -\mathrm{i}h_+(\alpha)\sigma_\alpha + g(\alpha)\tau_\alpha,
\end{aligned} \tag{6.10}$$

where

$$g(\alpha) = \frac{\kappa_1^+ \sinh^2(\alpha a) + \kappa_0^+ \alpha^2 a^2}{d(\alpha a)} - \frac{\kappa_1^- \sinh^2(\alpha b) + \kappa_0^- \alpha^2 b^2}{d(\alpha b)}, \tag{6.11}$$

$$h_\pm(\alpha) = \frac{\kappa_2^+(2\alpha a \pm \sinh(2\alpha a))}{d(\alpha a)} + \frac{\kappa_2^-(2\alpha b \pm \sinh(2\alpha b))}{d(\alpha b)}, \tag{6.12}$$

$$\kappa_0^\pm = \frac{1}{2\mu_\pm}, \quad \kappa_1^\pm = \frac{1-2\nu_\pm}{2\mu_\pm}, \quad \kappa_2^\pm = \frac{1-\nu_\pm}{2\mu_\pm}.$$

Next, we consider the interface conditions (6.2). We introduce the unknown functions Ψ_1, Ψ_2 in such a way that

$$\begin{aligned}
&\tau_{xy}(x,0) = \alpha_{11}[u](x) + \alpha_{12}[v](x) + \Psi_1(x),\\
&\sigma_y(x,0) = \alpha_{12}[u](x) + \alpha_{22}[v](x) + \Psi_2(x), \quad |x| < \infty,
\end{aligned} \tag{6.13}$$

and note that supp $\Psi_j(x) \subset (-c,c)$, $j = 1, 2$. In terms of the Fourier transforms, Eq. (6.13) can be written as

$$\begin{aligned}
&\tau_\alpha = \alpha_{11}\chi_{1\alpha} + \alpha_{12}\chi_{2\alpha} + \Psi_{1\alpha},\\
&\sigma_\alpha = \alpha_{12}\chi_{1\alpha} + \alpha_{22}\chi_{2\alpha} + \Psi_{2\alpha},
\end{aligned} \tag{6.14}$$

where

$$\Psi_{j\alpha} = \int_{-c}^{c} \Psi_j(\xi)\,\mathrm{e}^{\mathrm{i}\alpha\xi}\,\mathrm{d}\xi, \quad j = 1,2. \tag{6.15}$$

Then, instead of $\chi_{1\alpha}$, $\chi_{2\alpha}$ in Eq. (6.14) we substitute expressions (6.10) which yield

$$\sigma_\alpha = \frac{-\mathrm{i}\alpha}{\Delta(\alpha)}\{(\alpha_{12}\mathrm{i}h_-(\alpha) + \alpha_{22}g(\alpha))\Psi_{1\alpha} + (\mathrm{i}\alpha - \mathrm{i}\alpha_{11}h_-(\alpha) - \alpha_{12}g(\alpha))\Psi_{2\alpha}\}, \tag{6.16}$$

$$\tau_\alpha = \frac{\mathrm{i}\alpha}{\Delta(\alpha)}\{(\alpha_{11}g(\alpha) + \alpha_{12}\mathrm{i}h_+(\alpha))\Psi_{2\alpha} - (\mathrm{i}\alpha + \alpha_{12}g(\alpha) + \alpha_{22}\mathrm{i}h_+(\alpha))\Psi_{1\alpha}\}, \tag{6.17}$$

where

$$\begin{aligned}
\Delta(\alpha) &= -[\alpha_{11}g(\alpha) + \alpha_{12}\mathrm{i}h_+(\alpha)][\alpha_{12}\mathrm{i}h_-(\alpha) + \alpha_{22}g(\alpha)] - [\mathrm{i}\alpha + \alpha_{12}g(\alpha) + \alpha_{22}\mathrm{i}h_+(\alpha)]\\
&\quad \times [\mathrm{i}\alpha - \alpha_{11}\mathrm{i}h_-(\alpha) - \alpha_{12}g(\alpha)]\\
&= \alpha^2 + \{g^2(\alpha) + h_+(\alpha)h_-(\alpha)\}\{\alpha_{12}^2 - \alpha_{11}\alpha_{22}\} + \alpha_{22}\alpha h_+(\alpha) - \alpha_{11}\alpha h_-(\alpha).
\end{aligned} \tag{6.18}$$

Applying the inverse Fourier transform, using Eq. (6.15) and changing the order of integration we get the integral representations of traction components

$$\begin{aligned}
&\tau(x) = \int_{-c}^{c} \{\Psi_1(\xi)l_{11}(\xi - x) + \Psi_2(\xi)l_{12}(\xi - x)\}\,\mathrm{d}\xi,\\
&\sigma(x) = \int_{-c}^{c} \{\Psi_1(\xi)l_{21}(\xi - x) + \Psi_2(\xi)l_{22}(\xi - x)\}\,\mathrm{d}\xi, \quad |x| < \infty,
\end{aligned} \tag{6.19}$$

where

$$l_{kj}(t)=\frac{1}{2\pi}\int_{-\infty}^{\infty}p_{kj}(\alpha)\,\mathrm{e}^{\mathrm{i}\alpha t}\,\mathrm{d}\alpha, \tag{6.20}$$

$$\begin{aligned}
p_{11}(\alpha)&=\frac{\alpha^2}{\Delta(\alpha)}\Big\{1+\frac{\alpha_{12}}{\mathrm{i}\alpha}g(\alpha)+\frac{\alpha_{22}}{\alpha}h_+(\alpha)\Big\},\\
p_{12}(\alpha)&=\frac{\mathrm{i}\alpha}{\Delta(\alpha)}\{\alpha_{11}g(\alpha)+\alpha_{12}\mathrm{i}h_+(\alpha)\},\\
p_{21}(\alpha)&=\frac{-\mathrm{i}\alpha}{\Delta(\alpha)}\{\alpha_{12}\mathrm{i}h_-(\alpha)+\alpha_{22}g(\alpha)\},\\
p_{22}(\alpha)&=\frac{\alpha^2}{\Delta(\alpha)}\Big\{1-\frac{\alpha_{11}}{\alpha}h_-(\alpha)-\frac{\alpha_{12}}{\mathrm{i}\alpha}g(\alpha)\Big\}.
\end{aligned} \tag{6.21}$$

Considering the system (6.19) on the interval $(-c,c)$ and using Eq. (6.1) we obtain the system of integral equations

$$\sum_{j=1}^{2}\int_{-c}^{c}\Psi_j(\xi)l_{kj}(\xi-x)\,\mathrm{d}\xi=f_k(x),\quad k=1,2,\quad |x|<c. \tag{6.22}$$

6.2. Analysis of the system of integral equations

First, we analyse the asymptotic behaviour of the kernel functions $l_{jk}(\xi-x)$ as $\xi\to x$. We note that $l_{jk}(t)$ are singular at $t=0$. To obtain the structure of the singular terms, we need the asymptotics of the functions $p_{km}(\alpha)$ (see Eq. (6.20)) as $\alpha\to 0$ or $\alpha\to\infty$. Direct calculations show that

$$\begin{aligned}
g(\alpha)&\sim\frac{6}{\alpha^2}\left(\frac{\kappa_2^+}{a^2}-\frac{\kappa_2^-}{b^2}\right),\\
h_+(\alpha)&\sim\frac{12}{\alpha^3}\left(\frac{\kappa_2^+}{a^3}+\frac{\kappa_2^-}{b^3}\right),\\
h_-(\alpha)&\sim-\frac{4}{\alpha}\left(\frac{\kappa_2^+}{a}+\frac{\kappa_2^-}{b}\right),
\end{aligned}$$

as $\alpha\to 0$.

It follows from Eqs. (6.18) and (6.21) that

$$\Delta(\alpha)=\mathrm{O}(\alpha^{-4}),\quad \alpha\to 0$$

and

$$\begin{aligned}
&p_{11}(\alpha)=\mathrm{O}(\alpha^2),\quad p_{12}(\alpha)=\mathrm{O}(\alpha^2),\\
&p_{21}(\alpha)=\mathrm{O}(\alpha^3),\quad p_{22}(\alpha)=\mathrm{O}(\alpha^3),\quad \alpha\to 0.
\end{aligned} \tag{6.23}$$

The relationships (6.23) provide the convergence of the integrals (6.20) in the vicinity of $\alpha=0$, uniformly with respect to t. On the other hand, at infinity we have

$$g(\alpha)\sim\Lambda_-,\quad h_+(\alpha)\sim\pm\Lambda_+,\quad h_-(\alpha)\sim\mp\Lambda_+,\quad \alpha\to\pm\infty,$$

where

$$\Lambda_+=2(\kappa_2^++\kappa_2^-),\quad \Lambda_-=\kappa_1^+-\kappa_1^-.$$

The function $\Delta(\alpha)$ is characterised by

$$\Delta(\alpha) \sim \alpha^2 + (\alpha_{11} + \alpha_{22})\Lambda_+|\alpha| + (\Lambda_+^2 - \Lambda_-^2)(\alpha_{11}\alpha_{22} - \alpha_{12}^2), \quad \alpha \to \pm\infty.$$

Hence, the functions p_{kj} possess the asymptotics

$$p_{11}(\alpha) = 1 + \frac{\alpha_{12}}{\mathrm{i}\alpha}\Lambda_- - \frac{\alpha_{11}}{|\alpha|}\Lambda_+ + \mathrm{O}\left(\frac{1}{\alpha^2}\right),$$
$$p_{22}(\alpha) = 1 - \frac{\alpha_{12}}{\mathrm{i}\alpha}\Lambda_- - \frac{\alpha_{22}}{|\alpha|}\Lambda_+ + \mathrm{O}\left(\frac{1}{\alpha^2}\right),$$
$$p_{12}(\alpha) = \frac{\mathrm{i}\alpha_{11}}{\alpha}\Lambda_- - \frac{\alpha_{12}}{|\alpha|}\Lambda_+ + \mathrm{O}\left(\frac{1}{\alpha^2}\right),$$
$$p_{21}(\alpha) = -\frac{\mathrm{i}\alpha_{22}}{\alpha}\Lambda_- - \frac{\alpha_{12}}{|\alpha|}\Lambda_+ + \mathrm{O}\left(\frac{1}{\alpha^2}\right).$$

Taking into account the relationship

$$\frac{1}{2\pi}\int_{-\infty}^{\infty} \mathrm{e}^{\mathrm{i}\alpha t}\,\mathrm{d}\alpha = \delta(t),$$

where $\delta(t)$ is the delta function, we obtain

$$l_{kk}(t) = \delta(t) + l_{kk}^0(t), \quad k = 1, 2,$$

where

$$l_{kk}^0(t) = \frac{1}{2\pi}\int_{-\infty}^{\infty} p_{kk}^0(\alpha)\,\mathrm{e}^{\mathrm{i}\alpha t}\,\mathrm{d}\alpha,$$
$$p_{kk}^0(\alpha) = p_{kk}(\alpha) - 1.$$

We note that $l_{11}^0(t)$, $l_{22}^0(t)$, $l_{12}(t)$, $l_{21}(t)$ have logarithmic singularities as $t \to 0$. To obtain the logarithmic terms explicitly, we write

$$l_{11}^0(t) = \frac{1}{2\pi}\int_{-\infty}^{\infty} p_{11}^0\,\mathrm{e}^{\mathrm{i}\alpha t}\,\mathrm{d}\alpha$$
$$= \frac{1}{2\pi}\int_{-1}^{1} p_{11}^0\,\mathrm{e}^{\mathrm{i}\alpha t}\,\mathrm{d}\alpha + \frac{1}{2\pi}\int_L \left(p_{11}^0 - \frac{\alpha_{12}}{\mathrm{i}\alpha}\Lambda_- + \frac{\alpha_{11}}{|\alpha|}\Lambda_+\right)\mathrm{e}^{\mathrm{i}\alpha t}\,\mathrm{d}\alpha + \frac{1}{2\pi}\int_L \left(\frac{\alpha_{12}}{\mathrm{i}\alpha}\Lambda_- - \frac{\alpha_{11}}{|\alpha|}\Lambda_+\right)\mathrm{e}^{\mathrm{i}\alpha t}\,\mathrm{d}\alpha,$$

where $L = (-\infty, -1) \cup (1, +\infty)$. The first two integrals in the right-hand side converge uniformly for all real t, whereas the last integral diverges at $t = 0$. Namely,

$$\frac{1}{2\pi}\int_L \frac{\mathrm{e}^{\mathrm{i}\alpha t}}{\mathrm{i}\alpha}\,\mathrm{d}\alpha = \frac{1}{\pi}\operatorname{sgn} t\int_{|t|}^{\infty}\frac{\sin\tau}{\tau}\,\mathrm{d}\tau = -\frac{1}{\pi}\operatorname{sgn} t\,\mathrm{si}(|t|),$$

$$\frac{1}{2\pi}\int_L \frac{\mathrm{e}^{\mathrm{i}\alpha t}}{|\alpha|}\,\mathrm{d}\alpha = \frac{1}{\pi}\int_{|t|}^{\infty}\frac{\cos\tau}{\tau}\,\mathrm{d}\tau = -\frac{1}{\pi}\mathrm{ci}(|t|),$$

where $\mathrm{si}(x)$, $\mathrm{ci}(x)$ are the sine and cosine integral functions

$$\mathrm{si}(x) = -\frac{\pi}{2} + \sum_{k=1}^{\infty} \frac{(-1)^{k+1} x^{2k-1}}{(2k-1)(2k-1)!},$$

$$\mathrm{ci}(x) = \gamma + \log|x| + \sum_{k=1}^{\infty} \frac{(-1)^{k} x^{2k}}{2k(2k)!},$$

and γ is the Euler constant. Thus,

$$l_{11}(t) = \delta(t) + \frac{1}{\pi}\alpha_{11}\Lambda_{+}\log|t| + \frac{1}{2}\alpha_{12}\Lambda_{-}\mathrm{sgn}\, t + \tilde{l}_{11}(t),$$

where $\tilde{l}_{11}(t)$ is continuous on the whole real axis. In a similar way,

$$l_{22}(t) = \delta(t) + \frac{1}{\pi}\alpha_{22}\Lambda_{+}\log|t| - \frac{1}{2}\alpha_{12}\Lambda_{-}\mathrm{sgn}\, t + \tilde{l}_{22}(t),$$

$$l_{12}(t) = \frac{1}{\pi}\alpha_{12}\Lambda_{+}\log|t| - \frac{1}{2}\alpha_{11}\Lambda_{-}\mathrm{sgn}\, t + \tilde{l}_{12}(t),$$

$$l_{21}(t) = \frac{1}{\pi}\alpha_{12}\Lambda_{+}\log|t| + \frac{1}{2}\alpha_{22}\Lambda_{-}\mathrm{sgn}\, t + \tilde{l}_{21}(t),$$

where the functions $\tilde{l}_{kj}(t)$ are continuous. Hence, the system (6.22) can be written in the form

$$\Psi_k(cx) + c\sum_{j=1}^{2}\int_{-1}^{1}\left\{\frac{\beta_{kj}}{\pi}\log|\xi - x| + \mathscr{K}_{kj}(\xi - x)\right\}\Psi_j(c\xi)\,\mathrm{d}\xi = f_k(cx), \quad |x| < 1, \quad k = 1,2, \tag{6.24}$$

which is a Fredholm system of the second kind. Here

$$\mathscr{K}_{kj}(t) = \frac{\beta_{kj}}{\pi}\log c + \frac{1}{2\pi}\int_{-\infty}^{\infty} p^{1}_{kj}(\alpha)\,\mathrm{e}^{\mathrm{i}\alpha tc}\,\mathrm{d}\alpha + \frac{(-1)^{k}}{\pi}\eta_{kj}\,\mathrm{sgn}\, t\,\mathrm{si}(c|t|) + \frac{\beta_{kj}}{\pi}\left(\gamma + \sum_{s=1}^{\infty}\frac{(-1)^{s}(ct)^{2s}}{2s(2s)!}\right),$$

$$p^{1}_{kj}(\alpha) = p_{kj}(\alpha) - \delta_{kj} + \frac{(-1)^{k}\eta_{kj}}{\mathrm{i}\alpha}\varepsilon(\alpha) + \frac{\beta_{kj}\varepsilon(\alpha)}{|\alpha|},$$

$$\varepsilon = \begin{cases} 1, & |\alpha| > 1 \\ 0, & |\alpha| < 1, \end{cases}$$

$$\beta_{kj} = \alpha_{kj}\Lambda_{+},$$

$$\eta_{11} = \alpha_{12}\Lambda_{-}, \quad \eta_{12} = \alpha_{11}\Lambda_{-},$$

$$\eta_{21} = \alpha_{22}\Lambda_{-}, \quad \eta_{22} = \alpha_{12}\Lambda_{-}.$$

We note that $p^{1}_{kj}(\alpha) = \mathrm{O}(\alpha^{-2})$ as $\alpha \to \pm\infty$.

To prove the boundedness of the solution at the point $x = 1$ we admit an integrable singularity for the functions $\Psi_k(cx)$ at this point

$$\Psi_k(cx) \sim \mathscr{N}_k(1-x)^{\alpha}, \quad x \to 1-0; \quad -1 < \alpha < 0. \tag{6.25}$$

The behaviour of the integral with the logarithmic kernel at the end $x = 1$ is described by

$$\int_{-1}^{1}\log|y-x|(1-y)^{\alpha}\,\mathrm{d}y = \frac{\pi\cot\pi\alpha}{\alpha+1}(1-x)^{\alpha+1} + \phi(x;\alpha), \quad x \to 1-0, \tag{6.26}$$

where $\phi(x;\alpha)$ is bounded in the neighbourhood of the point $x=1$. Then we substitute formulae (6.25) and (6.26) into Eq. (6.24)

$$\mathscr{N}_k(1-x)^{\alpha}+c\sum_{j=1}^{N}\left\{\beta_{kj}\frac{\cot\pi\alpha}{\alpha+1}\mathscr{N}_j(1-x)^{\alpha+1}+\phi_{kj}(x;\alpha)\right\}=f_k(cx),\quad x\to 1-0,$$

where $\phi_{kj}(x;\alpha)$ are bounded as $x\to 1$. The left hand-sides of the last equations are bounded if and only if $\mathscr{N}_1=\mathscr{N}_2=0$. It means that the functions $\Psi_k(cx)$ may possess logarithmic singularities or be bounded at the end $x=1$. Again, we admit

$$\Psi_k(cx)\sim M_k\ln(1-x),\quad x\to 1-0$$

and take into account the behaviour of the integral

$$\int_{-1}^{1}\log|y-x|\log(1-y)\,\mathrm{d}y=C(1-x)\ln(1-x)+\phi_0(x),\quad x\to 1-0 \tag{6.27}$$

where C is a constant and $\phi_0(x)$ is a bounded function as $x\to 1$. In a similar way, system (6.24) and formula (6.27) give $M_1=M_2=0$.

Thus, this analysis shows that the functions $\Psi_1(cx)$, $\Psi_2(cx)$ possess neither logarithmic nor power singularities at the end $x=1$ and $x=-1$ (obviously, the analysis of the functions Ψ_1, Ψ_2 at the point $x=-1$ is similar to the previous one for $x=1$), i.e. the solution of (6.24) is bounded at the ends of the interval $(-1,1)$. Moreover, if we take into account the interface conditions (6.13), the traction conditions (6.1) and the system (6.24), we find that the displacement jumps $\chi_1(x)=[u](x)$, $\chi_2(x)=[v](x)$ are continuous at the points $x=\pm c$ and the stress components $\sigma_y(x,0)$, $\tau_{xy}(x,0)$ are bounded and discontinuous at the ends $x=\pm c$.

7. Discussion and numerical results

First, we summarise the results of the analysis of the scalar formulations (see Sections 3–5) associated with the heat transfer problems (or anti-plane shear). We have presented the exact solutions of problems on cracks along imperfect interface boundaries. The authors are not aware of similar results published in the literature relevant to this work. The asymptotic analysis shows that the solution (the temperature or the transverse displacement) is bounded and its tangential derivative is characterised by a weak logarithmic singularity at the crack tip; the normal derivative of the solution is bounded. The behaviour of temperature (or displacement jump) at infinity depends on the geometry of the whole domain and the type of boundary conditions on the exterior contour. We have shown that the case of an infinite plane is qualitatively different from the cases involving a strip with a crack: in the latter case the solution is either bounded or decays exponentially at infinity, whereas for the problem involving an infinite two-phase plane we deal with power asymptotic expansions at infinity. In particular, the constant A in formula (4.10) has been evaluated explicitly to characterise the displacement (or temperature) jump at infinity along the crack when the Neumann boundary conditions are specified on the upper and lower boundaries of the strip. This problem can be considered as a model boundary layer formulation for a singularly perturbed domain involving a crack in a thin rectangle.

Next, we analyse a plane elasticity problem for a two-phase strip with a finite crack. A numerical solution is presented for the system (6.24). The numerical algorithm employed here is described in the Appendix.

The elastic layers are characterised by the Young's moduli $E_{\pm}$ and by the values $\nu_{\pm}$ of the Poisson ratio. By $\lambda_{\pm}$, $\mu_{\pm}$, we denote the Lamé constants of the elastic materials given by

$$\lambda_{\pm} = \frac{E_{\pm} v_{\pm}}{(1+v_{\pm})(1-2v_{\pm})}, \quad \mu_{\pm} = \frac{E_{\pm}}{2(1+v_{\pm})},$$

and

$$\lambda = \frac{E_0 v_0}{(1+v_0)(1-2v_0)}, \quad \mu = \frac{E_0}{2(1+v_0)}$$

are the normalised Lamé constants related to the middle layer. For all the tests we considered the upper material to be aluminium with the following elastic moduli (see Adams et al., 1997)

$$E_{+(\mathrm{Al})} = 70 \text{ GPa}; \quad v_{+(\mathrm{Al})} = 0.3.$$

The lower material can be either aluminium, CFRP or brass, the last two having the following elastic moduli

$$E_{-(\mathrm{CFRP})} = 135 \text{ GPa}; \quad v_{-(\mathrm{CFRP})} = 0.3,$$

$$E_{-(\mathrm{Br})} = 100 \text{ GPa}; \quad v_{-(\mathrm{Br})} = 0.25.$$

The interface layer is assumed to be made of FM 1000 and characterised by the normalised moduli,

$$E = 10 \text{ GPa}; \quad v = 0.4$$

whereas the real values are given by

$$E_0 = 1.24 \text{ GPa}; \quad v_0 = 0.41,$$

and thus here $\epsilon = 0.124$. The parameters that are involved in the interface condition in this case have the following values,

$$\alpha_{11} = 0.35 \text{ GPa}; \quad \alpha_{22} = 2.3 \text{ GPa},$$

and by the approximation (2.11) (see Appendix), $\alpha_{12} = \alpha_{21} = 0$.

Several cases of applied load are considered and listed in the Tables 1 and 2.

Table 1
Symmetric case ($a = b = c = 1$)

Case	Type of load	Lower layer
A.1	$f_1 = 0; f_2 = -1$	CFRP
A.2	$f_1 = 0; f_2 = -1$	Brass
A.3	$f_1 = 1; f_2 = 0$	CFRP
A.4	$f_1 = 1; f_2 = 0$	Brass

Table 2
Combined effect ($f_1 = 1; f_2 = 0$)

Case	Geometry	Lower layer
B.1	$a = c = 1; b = 100$	Aluminium
B.2	$a = b = c = 1$	Aluminium
B.3	$a = c = 1; b = 100$	Brass
B.4	$a = b = c = 1$	Brass

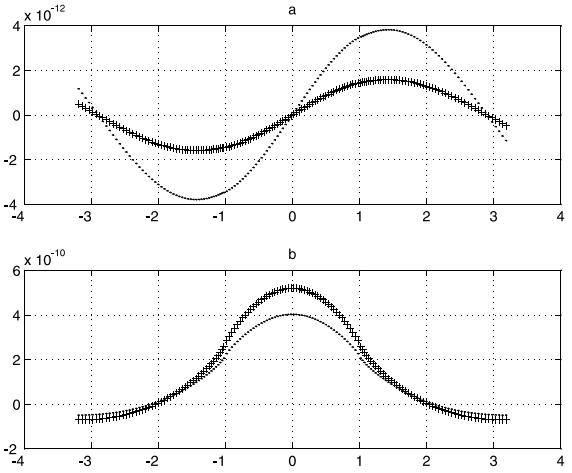

Fig. 7. The displacement jump versus x for $a = b = 1$, $c = 1$ in the cases ($f_1 = 0$, $f_2 = -1$): A.1 (Al, CFRP); A.2 (Al, Br). a. ($\cdots$) $[u]$ (A.1); ($+ + +$) $[u]$ (A.2); b. ($\cdots$) $[v]$ (A.1); ($+ + +$) $[v]$ (A.2).

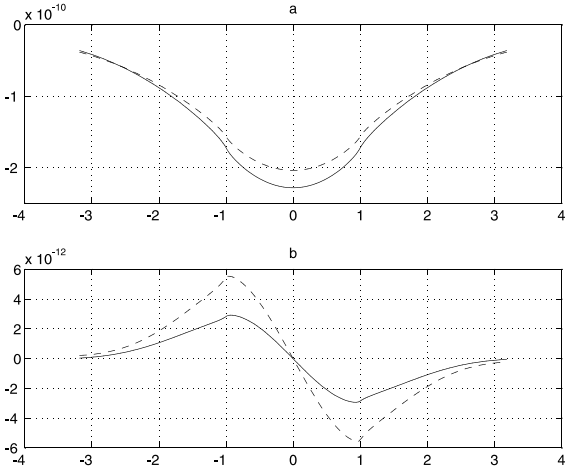

Fig. 8. The displacement jump versus x for $a = b = 1$, $c = 1$ in the cases ($f_1 = 1$, $f_2 = 0$): A.3 (Al, CFRP); A.4 (Al, Br). a. ($- - -$) $[u]$ (A.3); (—) $[u]$ (A.4); b. ($- - -$) $[v]$ (A.3); (—) $[v]$ (A.4).

Figs. 7 and 8 include the graphs of the displacement jump components evaluated for the symmetric structure involving the elastic layers of the same thickness.

The results are presented for the normal and shear external loads and different values of elastic moduli. We note that the negative values of the vertical displacement jump correspond to overlapping of the phases on the imperfect interface. This is a consequence of the linearisation of the model. However, both negative and positive values of the tangential displacement jump presented in Figs. 7 and 8 make sense physically. It is noted that the displacement jump is continuous in the vicinity of the crack ends.

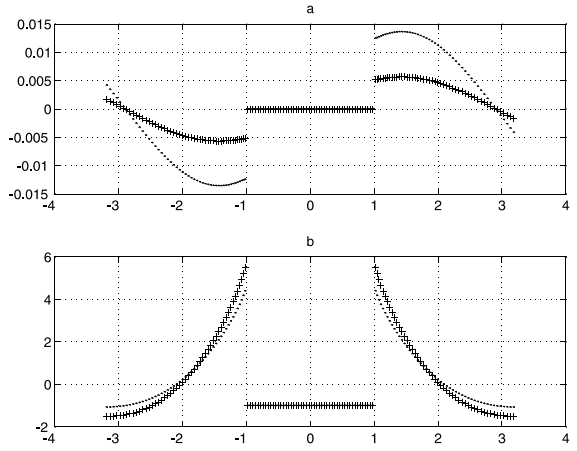

Fig. 9. The stress components along the interface versus x for $a = b = 1$, $c = 1$. a. $(\cdots)$ τ_{xy} (A.1); $(+++)$ τ_{xy} (A.2); b. $(\cdots)$ σ_y (A.1); $(+++)$ σ_y (A.2).

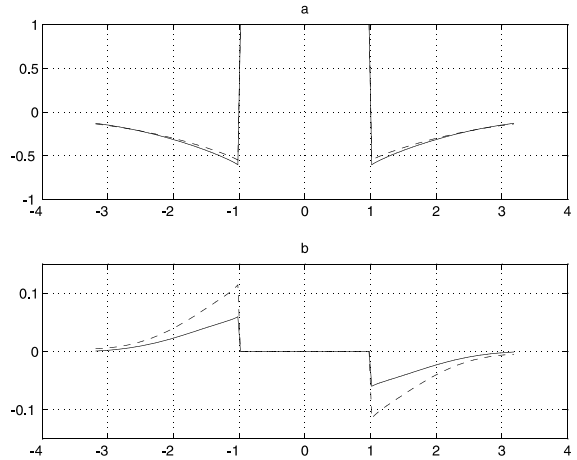

Fig. 10. The stress components along the interface versus x for $a = b = 1$, $c = 1$. a. $(---)$ τ_{xy} (A.3); (—) τ_{xy} (A.4); b. $(---)$ σ_y (A.3); (—) σ_y (A.4).

The corresponding graphs for stress are given in Figs. 9 and 10. As predicted the stress components $\sigma_y(x,0)$, $\tau_{xy}(x,0)$ are bounded and discontinuous at the ends of the crack.

Figs. 11 and 12 show the graphs of displacement and traction components for the case of layers of different thickness and elastic moduli. Only shear load cases are considered. It is observed that the longitudinal displacement jump takes its maximum value for the case of a symmetric strip when both layers have the same thickness and elastic moduli.

The examples presented above are given for the purpose of illustration yet our algorithm has been designed for a general smooth load and can take into account a wide variety of geometric parameters of the structure. The interface layer can be anisotropic.

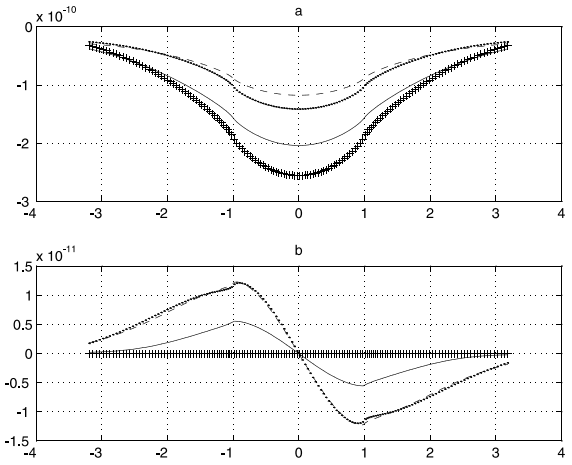

Fig. 11. The displacement jump versus x for $f_1 = 1$, $f_2 = 0$, $c = 1$ in the cases (Al, Al): B.1 (a = 1, b = 100); B.2 (a = b = 1); and (Al, Br): B.3 (a = 1, b = 100); B.4 (a = b = 1). a. $(\cdots)$ $[u]$ (B.1); $(+\,+\,+)$ $[u]$ (B.2); $(-\,-\,-)$ $[u]$ (B.3); (—) $[u]$ (B.4); b. $(\cdots)$ $[v]$ (B.1); $(+\,+\,+)$ $[v]$ (B.2); $(-\,-\,-)$ $[v]$ (B.3); (—) $[v]$ (B.4).

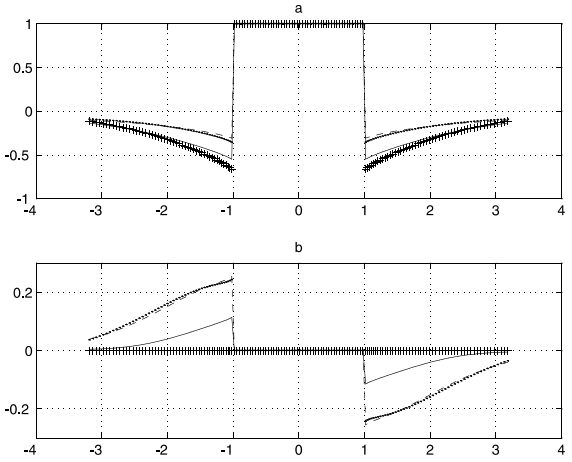

Fig. 12. The stress components along the interface versus x for $f_1 = 1$, $f_2 = 0$ a. $(\cdots)$ τ_{xy} (B.1); $(+\,+\,+)$ τ_{xy} (B.2); $(-\,-\,-)$ τ_{xy} (B.3); (—) τ_{xy} (B.4); b. $(\cdots)$ σ_y (B.1); $(+\,+\,+)$ σ_y (B.2); $(-\,-\,-)$ σ_y (B.3); (—) σ_y (B.4).

Acknowledgements

The work was supported by UK Engineering and Physics Sciences Research Counsil (EPSRC), grant no./ GR/k76634. Financial support from CONACyT-ORS Award and the University of Bath is fully acknowledged.

Appendix A

Here we present a brief description of the numerical approach that we use for the system (6.24) that is a Fredholm system of integral equations of the second kind.

Writing

$$\Psi(cx_n) = A_n^{(k)}, \quad k = 1,2, \quad n = 1,2,\ldots,N,$$
$$x_n = -1 + \frac{2n-1}{N}, \quad n = 1,2,\ldots,N,$$
$$y_n = -1 + \frac{2n}{N}, \quad n = 0,1,\ldots,N,$$

one can discretise the system (6.24) as follows:

$$\Psi_k(cx_n) + c\sum_{j=1}^{2}\sum_{m=1}^{N}\int_{y_{m-1}}^{y_m}\left\{\frac{\beta_{kj}}{\pi}\ln|\xi - x_n| + \mathcal{K}_{kj}(\xi - x_n)\right\}\mathrm{d}\xi\Psi_j(cx_m) = f_k(cx_n).$$

Thus, we arrive at the following linear system of algebraic equations

$$A_n^{(k)} + c\sum_{j=1}^{2}\sum_{m=1}^{N}\mathscr{D}_{nm}^{(k,j)}A_m^{(j)} = c_n^{(k)}, \quad k = 1,2; \quad n = 1,2,\ldots,N \tag{A.1}$$

where the coefficients $\mathscr{D}_{nm}^{(k,j)}$ and $c_n^{(k)}$ are given by

$$\mathscr{D}_{nm}^{(k,j)} = \int_{y_{m-1}}^{y_m}\left[\frac{\beta_{kj}}{\pi}\ln|\xi - x_n| + \mathcal{K}_{kj}(\xi - x_n)\right]\mathrm{d}\xi \tag{A.2}$$

$$c_n^{(k)} = f_k(cx_n), \quad k = 1,2.$$

Direct calculations show that Eq. (A.2) can be written in the following way:

$$\mathscr{D}_{nm}^{(k,j)} = \frac{\beta_{kj}}{\pi}[(x_n - y_{m-1})(\ln|x_n - y_{m-1}| - 1) - (x_n - y_m)(\ln|x_n - y_m| - 1)] + \frac{2\log c}{\pi N}\beta_{kj} + \frac{1}{\pi}\int_{-\infty}^{\infty}Q(\alpha)\,\mathrm{d}\alpha$$
$$+ \frac{(-1)^k\eta_{kj}}{\pi}\left[\frac{\pi}{N}W_{mn} + S_1\right] + \frac{\beta_{kj}}{\pi}\left[\frac{2\gamma}{N} + S_2\right],$$

where

$$S_1 = \sum_{s=1}^{\infty}\frac{(-1)^{s+1}c^{2s-1}\left[(y_m - x_n)^{2s} - (y_{m-1} - x_n)^{2s}\right]}{(2s-1)(2s)!}$$

$$S_2 = \sum_{s=1}^{\infty}\frac{(-1)^{s}c^{2s}\left[(y_m - x_n)^{2s+1} - (y_{m-1} - x_n)^{2s+1}\right]}{2s(2s+1)!}$$

$$Q(\alpha) = \left\{p_{kj}(\alpha) - \delta_{kj} + (-1)^k\eta_{kj}\frac{\varepsilon(\alpha)}{\mathrm{i}\alpha} + \beta_{kj}\frac{\varepsilon(\alpha)}{|\alpha|}\right\}\frac{\sin\left(\frac{\alpha c}{N}\right)}{\alpha}\,\mathrm{e}^{\mathrm{i}\alpha c(t_m - x_n)},$$

$$\delta_{kj} = \begin{cases}1, & k = j\\ 0, & k \neq j\end{cases},$$

$$W_{mn} = \begin{cases}1, & x_n > y_m\\ -1, & x_n < y_{m-1}\\ 0, & x_n \in (y_{m-1}, y_m)\end{cases},$$

$$t_m = -1 + \frac{2m-1}{N}.$$

The value of $\int_{-\infty}^{\infty} Q(\alpha)\,\mathrm{d}\alpha$ can be obtained by using any numerical procedure. Here we use the trapezoidal method. It is worth to mention that $Q(\alpha) \in L_1(-\infty,+\infty)$ and $Q(\alpha) = \mathrm{O}\left(\frac{1}{\alpha^3}\right)$ as $\alpha \to \pm\infty$. The structure of the functions $p_{kj}(\alpha)$, $\Delta(\alpha), g(\alpha)$ and $h_{\pm}(\alpha)$ (see Eqs. (6.11), (6.12), (6.18) and (6.21)) allows us to write them in the form,

$$p_{kj}(\alpha) = p^{\mathrm{e}}_{kj}(\alpha) + \mathrm{i}p^{\mathrm{o}}_{kj}(\alpha), \tag{A.3}$$

where the real functions p^{e}_{kj} are even and the real functions p^{o}_{kj} are odd,

$$\begin{aligned}
&p^{\mathrm{e}}_{11}(\alpha) = \tfrac{\alpha^2}{\Delta(\alpha)}\left[\tfrac{\alpha_{22}}{\alpha}h_+(\alpha)+1\right]; \quad p^{\mathrm{o}}_{11}(\alpha) = -\tfrac{\alpha}{\Delta(\alpha)}\alpha_{12}g(\alpha)\\
&p^{\mathrm{e}}_{12}(\alpha) = -\tfrac{\alpha}{\Delta(\alpha)}\alpha_{12}h_+(\alpha); \quad p^{\mathrm{o}}_{12}(\alpha) = \tfrac{\alpha}{\Delta(\alpha)}\alpha_{11}g(\alpha)\\
&p^{\mathrm{e}}_{21}(\alpha) = \tfrac{\alpha}{\Delta(\alpha)}\alpha_{12}h_-(\alpha); \quad p^{\mathrm{o}}_{21}(\alpha) = -\tfrac{\alpha}{\Delta(\alpha)}\alpha_{22}g(\alpha)\\
&p^{\mathrm{e}}_{22}(\alpha) = \tfrac{\alpha^2}{\Delta(\alpha)}[1-\tfrac{\alpha_{11}}{\alpha}h_-(\alpha)]; \quad p^{\mathrm{o}}_{22}(\alpha) = \tfrac{\alpha}{\Delta(\alpha)}\alpha_{12}g(\alpha)
\end{aligned}$$

Thus, it turns out can that all the values $\mathscr{D}^{(k,j)}_{nm}$ in the system (A.1) are real. We substitute (A.3) into the relationship for $Q(\alpha)$ and obtain

$$\int_{-\infty}^{\infty} Q(\alpha)\,\mathrm{d}\alpha = 2\int_0^{\infty} Q_+(\alpha)\,\mathrm{d}\alpha,$$

where

$$Q_+(\alpha) = \left\{\left[p^{\mathrm{e}}_{kj}(\alpha) - \delta_{kj} + \beta_{kj}\frac{\varepsilon(\alpha)}{\alpha}\right]\cos c(x_m - x_n)\alpha + \left[-p^{\mathrm{o}}_{kj}(\alpha) + (-1)^k\eta_{kj}\frac{\varepsilon(\alpha)}{\alpha}\right]\sin c(x_m - x_n)\alpha\right\}\frac{\sin\left(\frac{\alpha c}{N}\right)}{\alpha}.$$

Once that the system (A.1) is solved we then can calculate the approximated values for the displacement jumps $[u](cx_n)$, $[v](cx_n)$ along the crack,

$$[u](cx_n) = \frac{1}{\alpha_*}\left\{\alpha_{22}[c^{(1)}_n - A^{(1)}_n] - \alpha_{12}[c^{(2)}_n - A^{(2)}_n]\right\},$$

$$[v](cx_n) = \frac{1}{\alpha_*}\left\{-\alpha_{12}[c^{(1)}_n - A^{(1)}_n] + \alpha_{11}[c^{(2)}_n - A^{(2)}_n]\right\},$$

where α_{11}, α_{12}, α_{21} and α_{22} are the same as in Section 6 (see Eq. (6.2)) and $\alpha_* = \alpha_{11}\alpha_{22} - \alpha^2_{12}$.

For $|x| > c$, the components of traction vector along the interface are

$$\tau_{xy} = f_1(x), \quad \sigma_y = f_2(x),$$

where

$$f_k(\pm cz_n) = c\sum_{j=1}^{2}\sum_{m=1}^{N} A^{(j)}_m \mathscr{D}^{(k,j)\pm}_{nm}, \tag{A.4}$$

and $\mathscr{D}^{(k,j)\pm}_{nm}$ coincides with $\mathscr{D}^{(k,j)}_{nm}$ when one substitutes x_n by $\pm z_n$, $z_n > 1$.

Finally, we can also find the displacement jumps outside the crack,

$$[u](\pm cz_n) = \frac{1}{\alpha_*}\{\alpha_{22}f_1(\pm cz_n) - \alpha_{12}f_2(\pm cz_n)\},$$

$$[v](\pm cz_n) = \frac{1}{\alpha_*}\{-\alpha_{12}f_1(\pm cz_n) + \alpha_{11}f_2(\pm cz_n)\}.$$

For all the calculations, the matrix α_{ij} is approximated by the matrix obtained in Eq. (2.11) by which it can be seen that $\alpha_{12} = \alpha_{21}$,

$$\alpha_{ij} = \begin{pmatrix} \alpha_{11} & \alpha_{12} \\ \alpha_{12} & \alpha_{22} \end{pmatrix} = \begin{pmatrix} \mu & 0 \\ 0 & \lambda + 2\mu \end{pmatrix}.$$

The quantities μ and λ are the normalised values of the elastic moduli for the adhesive joint treated in Section 2.

References

Adams, R.D., Comyn, J., Wake, W.C., 1997. Structural Adhesive Joints in Engineering, second ed.,. Chapman and Hall, London.

Antipov, Y.A., Kolaczkowski, S.T., Movchan, A.B., Spence, A., 2000. Asymptotic analysis for cracks in a catalytic monolith combustor. Int. J. Solids Struct. 37, 1899–1930.

Antipov, Y.A., 1993. An efficient solution of Prandtl-type integrodifferential equations in a section and its application to contact problems for a strip. J. Appl. Maths Mech. 57 (3), 547–556.

Avila-Pozos, O., Klarbring, A., Movchan, A.B., 1999. Asymptotic model of orthotropic highly inhomogeneous layered structure. Mech. Mater. 31, 101–115.

Bigoni, D., Ortiz, M., Needleman, A., 1997. Effect of interfacial compliance on bifurcation of a layer bonded to a substrate. Int. J. Solids Struct. 33–34, 4305–4326.

England, A.H., 1965. A crack between dissimilar media. Trans. ASME, Ser. E, J. Appl. Mech. 32, 400–402.

Gakhov, F.D., 1966. Boundary Value Problems, second ed. Addison-Wesley, Reading, MA.

Gradshteyn, I.S., Ryzhik, I.M., 1980. Table of integrals, series and products, fourth ed. Academic Press, New York.

Hayes, R.E., Kolaczkowski, S.T., 1997. Introduction to catalytic combustion. Gordon and Breach, New York.

Klarbring, A., 1991. Derivation of a model of adhesively bonded joints by the asymptotic expansion method. Int. J. Engng. Sci. 29 (4), 493–512.

Klarbring, A., Movchan, A.B., 1995. Asymptotic Analysis of Adhesively Bounded Joints. LiTH-IKP-R-848, Linköping University, Sweden.

Klarbring, A., Movchan, A.B., 1998. Asymptotic modelling of adhesive joints. Mech. Mater. 28, 137–145.

Noble, B., 1988. Methods based on the Wiener–Hopf technique: for the solution of partial differential equations. Chelsea Publishing Company.

Rice, J.R., Sih, G.C., 1965. Plane problems of cracks in dissimilar media. Trans. ASME, Ser. E, J. Appl. Mech. 32, 418–423.

Willis, J.R., 1971. Fracture mechanics of interfacial cracks. J. Mech. Phys. Solids 19, 353–368.